IEEE Access
Multidisciplinary ⋮ Rapid Review ⋮ Open Access Journal

Received 10 October 2022, accepted 23 October 2022, date of publication 26 October 2022, date of current version 3 November 2022.

Digital Object Identifier 10.1109/ACCESS.2022.3217504

RESEARCH ARTICLE

Modular Multi-Domain Aware Autonomous Surface Vehicle for Inspection

DANIEL FILIPE CAMPOS, ANÍBAL MATOS, (Member, IEEE), AND ANDRY MAYKOL PINTO

Faculty of Engineering, University of Porto, 4200-465 Porto, Portugal
Centre for Robotics and Autonomous Systems, INESC TEC, 4200-465 Porto, Portugal

Corresponding author: Daniel Filipe Campos (daniel.f.campos@inesctec.pt)

This work was supported in part by the Portuguese Government through the FCT—Foundation for Science and Technology within the Ph.D. Studentship to DC SFRH-BD-144263-2019, in part by the ERDF—European Regional Development Fund through the Operational Program for Competitiveness and Internationalization—COMPETE 2020 Program and FCT within Project POCI-01-0145-FEDER-030010 (DIIUS), and in part by the European Union's Horizon 2020—The EU Framework Program for Research and Innovation 2014–2020 under Grant 871571 (ATLANTIS).

ABSTRACT A growing interest in ocean exploration for scientific and commercial research has been shown, mainly due to the technological developments for maritime and offshore industries. The use of Autonomous surface vehicles (ASV) have a promising role to revolutionize the transportation, monitorization, operation and maintenance areas, allowing to perform distinct task from offshore assets inspection to harbor patrolling. This work presents SENSE, an autonomouS vEssel for multi-domaiN inSpection and maintEnance. It provides an open-source hardware and software architecture that is easy to replicate for both research institutes and industry. This is a multi-purpose vehicle capable of acquiring multi-domain data for inspecting and reconstructing maritime infrastructures. SENSE provides a research platform which can increase the situational awareness capabilities for ASVs. SENSE full configuration provides multimodal sensory data acquired from both domains using a Light Detection And Ranging (LiDAR), a stereoscopic camera, and a multibeam echosounder. In addition, it supplies navigation information obtained from a real-time kinematic satellite navigation system and inertial measurement units. Moreover, the tests performed at the harbor of *Marina de Leça*, at Porto, Portugal, resulted in a dataset which captures a fully operational harbor. It illustrates several conditions on maritime scenarios, such as undocking and docking examples, crossings with other vehicles and distinct types of moored vessels. The data available represents both domains of the maritime scenario, being the first public dataset acquired for multi-domain observation using a single vehicle. This paper also provides examples of applications for navigation and inspection on multi-domain scenarios, such as odometry estimation, bathymetric surveying and multi-domain mapping.

INDEX TERMS Maritime robotics, 3D perception, heterogeneous sensors, maritime dataset, multi-domain data.

I. INTRODUCTION

In the past two decades a growing interest in ocean exploration for scientific and commercial research has been shown, mainly due to the technological developments for maritime and offshore industries, which have provided major breakthroughs. Unmanned vehicles are becoming a key enabling technology for operating in challenging and hazardous areas at sea, accounting for the emerging of several tailor made solutions for different tasks from underwater vehicles to unmanned vessels.

The autonomous surface vehicles (ASV) technology is one research line in maritime robotics that can prove to be a powerful asset for a multitude of tasks, such as monitoring and surveying harbors, performing bathymetry and depth evaluations [1], and for the inspection and maintenance of offshore infrastructures, e.g. the transition pieces and scour protections of offshore wind farms [2]. Moreover, it can also

The associate editor coordinating the review of this manuscript and approving it for publication was Okyay Kaynak.

be used as a platform to perform preliminary tests on methodologies to be applied to autonomous ships for enhancing their situational awareness. For instance, tasks like docking, obstacle avoidance and mapping [3], [4], [5] could be validated on real maritime conditions, which otherwise would be rather difficult to validate at a real scale due to the legal constraints. With this manifold of research areas, the available ASVs are usually customized for a single application.

This work proposes an inspection and maintenance unmanned surface vehicle, the SENSE (autonomouS vEssel for multi-domaiN inSpection and maintEnance), that provides the versatility to adapt to the most suitable payload according to the task necessities. Furthermore, to improve the easiness of construction and replication, the SENSE is built with commercial off-the-shelf materials from standard trolling motors configured for differential drive to typically used sensors in multiple areas of maritime robotics. The version here presented is endowed with a sensor payload that allows the acquisition of multi-domain data, from the surface and underwater domains simultaneously. It uses a 3D LiDAR (Light Detection And Ranging), a stereoscopic camera and a multibeam echo sounder (MBES), as well as navigation sensors, namely GPS and IMU. The software is subdivided according to the modules in use and defines the control mode (remotely-operated or autonomous), acquires, processes and logs the sensors data and estimate the vehicle localization.

Therefore, the flexibility provided by SENSE offers the capability to adapt to different applications allowing to exchange the sensor payload, the available energy or the drive system by switching independent modules rather than redesigning the all system. This enhances the potential to be used as research platform and can be easily replicated by any other institution. Moreover, it can boost the development of cooperative ASVs with heterogeneous configurations using the same base design. The ROS-based software architecture allows a simple integration of new packages for researching new methodologies, such as global path planning [6], collision avoidance [7] and multi-domain mapping [8]. In parallel with the hardware customization, the SENSE provides a powerful development and testing platform for boosting the technology readiness level for the autonomy of ASVs, as well as a downscaled use case to validate situational awareness methods for autonomous ships.

The SENSE multi-domain perception capabilities enhances the observability and safety of the vehicle by representing the surface and underwater data. For instance, through multi-domain mapping it can create an unified representation of all maritime environment with the association of multimodal data acquired through heterogeneous sensors from both surface and underwater domains. This will generate information for increasing the perception capacity, which is crucial for multiple methodologies, such as collision avoidance and offshore inspection, as well as expand the exploration capabilities for maritime robotics.

Currently, the availability of datasets with multi-domain data in the literature is very limited and confidential. This lack of datasets along with the complexity of developing and deploying ASVs with multi-domain perception makes it more difficult to explore several open challenges for new situation awareness methodologies. Thus, the SENSE was used to gather the first publicly available dataset at the biggest yachting harbor in the north of Portugal, the ROAM@CRAS. It not only provides visual and 3D range data from the surface, 2D range underwater data, and navigation data from GPS and IMU, as also supplies an accurate positional ground-truth with centimetric precision. The available data illustrates the environmental challenges on the harbor use case scenario, from the weather and tidal effects on the vessel to the impact of crossings with larger vehicles and approaching big constructions. The ROAM@CRAS will enable the exploration of new state-of-the-art methods in the research areas of sensor fusion, multi-domain mapping and perception-based collision avoidance techniques, while in the presence of intermittent data, interactions with other vessels, static and dynamic features, and distinct navigational challenges from the harbor operations.

Therefore, the main contributions of this paper include:

- The design of a modular ASV, the SENSE, fitted to navigate on harbors and offshore infrastructures to acquire multi-domain data for inspection, surveying and mapping tasks;
- An open-source architecture for navigation and data acquisition given as a public repository from CRAS (Centre for Robotics and Autonomous Systems) at https://github.com/danielfbcampos/SENSE.git;
- The first dataset to provide data from both domains simultaneously in the maritime environment, surface and underwater, using a single vehicle, which otherwise would require several specialized vehicles. The ROAM@CRAS dataset provides ROS-Compliant information and is available as a public repository at https://rdm.inesctec.pt/dataset/nis-2020-002;
- A dataset to evaluate and mitigate several data fusion challenges, namely for odometry estimation and multi-domain mapping techniques. It presents real application challenges, such as waves from crossings with larger vehicles, navigation in close range to big structures, dynamic scenario and missing data.

This paper is organized as follows: Section II presents the related work, where some ASVs and datasets available in the scientific and industrial community are described. SENSE architecture is presented in Section III. Section IV depicts the ROAM@CRAS dataset, the data acquired from the SENSE and applications examples. Finally, the major conclusions of this work are discussed in Section V.

II. RELATED WORK

Several institutions, universities, industries and military started developing ASVs in the past two decades for multiple applications, such as oceanography, underwater surveying, bathymetry and maritime surveillance. Nowadays, most of the ASV technologies features limited autonomy,

sensor payloads and endurance [9]. This technology is mainly focused on experimental platforms, where some of them acquires perception data from the environment domains independently, namely from the surface domain or underwater domain. Nevertheless, several solutions are still deprived from perception sensors capable of providing observations of the surroundings, being designed only for navigation tests [10], environmental data collection [11] or as communication relays [12].

Currently, some commercial solutions are emerging, such as Teledyne Z-Boat 1250,[1] Kongsberg Geoswath 4R,[2] DriX [13], Seafloor Systems HydroCat-180[3] and Ocean Alpha ME120,[4] presenting products focused on the exploration of the underwater environment that are either remotely-operated or fully autonomous. In the research community, solutions that acquire perception data from a single domain are the most common with a higher focus on underwater surveying. The work of Bingham et al. [14] characterizes a wave glider capable of acquiring underwater data, such as animal detection and seafloor depth estimation, using passive and active acoustic sensors. Moreover,Beck et al. [15] developed a twin hull autonomous platform, the SeaWasp, for shallow water mapping using a multibeam sonar from Imagenex. The ROAZ, a catamaran ASV, proposed by Ferreira et al. [16] allows the acquisition of bathymetric data from shallow water environments and water-land interface zones using a Tritech echo sounder. Yang et al. [17] propose the USV-ZhengHe that uses cameras for monitoring and surveillance of inshore scenarios such as harbors. Groves et al. [18] proposes the MallARD ASV which allows the acquisition of 2D data from the surface using a two-dimensional laser scanner, mainly used for localizing the ASV in GPS-denied scenarios.

Some solutions enables the acquisition of data from both domains. Two available researches uses 3D point clouds from LiDAR solutions to observe the surface domain and multibeam echosounders to acquire information from the underwater domain, as described in the works of Leedekerken et al. [19] and Papadopoulos et al. [20]. Both works proposes a multi-domain mapping approach using a modified SCOUT robotic kayak with approximately 2.8 m length actuated by a single thruster. The vehicle for Leedekerken et al. [19] is endowed with GPS, IMU and DVL as navigation sensors, and three SICK LMS291 2D laser scanners, two 2D Hokuyo laser scanners mounted on a rotating shaft and a Blueview MB2250 imaging sonar for perceiving the surface and underwater domains. As for Papadopoulos et al. [20], the vehicle is also endowed with GPS, IMU and DVL, not used in this work, the same imaging sonar and the 3D LiDAR Velodyne HDL-64E.

[1]Teledyne, 2020. *Z-Boat 1250*. URL: https://tinyurl.com/ybapemnf

[2]Kongsberg, 2020. *Geoswath 4R*. URL: https://tinyurl.com/yccyazs7

[3]Seafloor Systems, 2020. *HydroCat-180*. URL: https://tinyurl.com/yde84mqy

[4]Ocean Alpha, 2020. *ME120*. URL: https://tinyurl.com/ydduhz7m

Nevertheless, besides most of the available technologies being mainly focused on single domain exploration (usually underwater), the exchange of components or sensor payload is constrained by either proprietary technology or requires a large engineering effort to replace. Moreover, some solutions offers large vehicles that makes the transportation and deployment more complex. Therefore, the design of a small, modular and multi-domain vehicle increases the flexibility to build one or several vehicles that can be quickly mission-ready that is capable of acquiring heterogeneous data using multimodal sensors, independently of the task requirements.

Thus, the SENSE contributes with a cost-effective solution that provides a platform for data acquisition from both domains and a modular vehicle that could easily be adapted with distinct sensor payloads to work for multiple maritime scenarios and purposes. This work contributes with a powerful tool to acquire multi-purpose datasets that can enhance the situational awareness and navigation capabilities for multiple applications, from offshore inspection to autonomous ships.

Moreover, currently datasets have become an important tool in the scientific and industrial communities to implement, validate and benchmark various techniques in multiple areas such as image analysis and sensor fusion [21]. This provides a major boost in the exploration of new techniques for maritime robotics with works for depth completion [22], [23], object recognition [24] and classification [25], obstacle detection [26] and the expansion of sensor capabilities [27]. Also, with the appearance of test beds, like the proposed on the ATLANTIS Test Center [28], its expected to increase the data availability and variability, strengthening the research for offshore inspection and improve the vehicles situational awareness.

Nowadays, no public dataset provides data from both domains of the maritime scenarios. In the past years, datasets have been more focused on autonomous driving [29], [30], [31], maritime image systems [26], [32], [33] and underwater sonar data [34], [35], [36]. In addition, existing datasets capturing marine environments for robotic applications are focused only on single domain observation, either on surface or underwater. On the surface domain, the data acquired is mainly used on applications such as maritime vehicle classification [37], maritime objects semantic segmentation [26], [32], [38] and dock detection and classification [39], [40]. For the underwater domain more datasets are available with applications such as acoustic measurements [34], [36], image enhancement and colorization [33], [41], [42], underwater SLAM [35], image segmentation [43] and object classification [24]. On Table 1 a summary of some relevant datasets is provided as example.

As such, the development of a multi-domain dataset will provide a contribution to explore and expand the situational awareness and 3D reconstruction capabilities to create multi-domain maps with methodologies such as proposed by Leedekerken et al. [19], Papadopoulos et al. [20] and Campos et al. [8]. This will increase the safety and the observability of the surroundings while reducing the

TABLE 1. Summary of some available datasets for surface or underwater scenarios.

Dataset	Environment	Ground-truth	Details
MARVEL [44]	Surface	✓	- Image data - Maritime vessel images - Vessel classification
MaSTr1325 [38]	Surface	✓	- Stereo image data - Multiple weather conditions - Obstacle segmentation and detection
Dora@CRAS [39]	Surface	✓	- Image data - Point cloud data - Simulation - Dock detection
Five-Element Acoustic [34]	Underwater	✓	- Sonar data - ASV mount - Bathymetry
Underwater Caves [36]	Underwater	✓	- Sonar data - Underwater cave mapping - ROS based
Afonso [24]	Underwater	✓	- Image data - Different turbidity - Object classification
Li [33]	Underwater	✓	- Image data - Various turbidity and colorization - Image enhancement

necessity for multiple vehicles operating in the same zones.

III. SENSE AUTONOMOUS SURFACE VEHICLE

A. MECHANICAL DESCRIPTION

The SENSE is a small sized ASV with 1.5 m length, approximately 50 kg, 2 h operation time and differential drive. It uses commercial off-the-shelf materials to be a cost-effective platform that can be easily replicated by universities, research centres and companies. The structural construction is based on the INESC TECs' Zarco ASV [45] and is composed by anodized aluminium profiles linked to each other to form the rigid frame which can be attached to two polyethylene pontoons with snap buttons, creating the flotation system for the catamaran configuration. Each pontoon provides a net buoyancy of 50 kg. Thus, with the minimal configuration, energy and navigation modules, the SENSE weights approximately 50 kg providing an extra 50 kg for any additional payload. The flotation system will affect the maximum velocities and the operational limits, where bulkier pontoons with higher stability, as used currently in SENSE, will reach lower velocities while thinner pontoons will provide higher speed at cost of lower stability. The operation requirements for SENSE to operate corresponds to wind state 2 (light breeze) and sea state 3 (small wavelets) in the Beaufort Scale,[5] requiring favourable conditions to operate, such as found in the Mediterranean Sea during Summer time. In Table 2 a summary of the SENSE characteristics is presented, where the total weight, additional payload and operation time corresponds to the minimal configuration (energy and navigation modules only).

TABLE 2. Technical specifications of the SENSE.

Characteristics	Specifications
Dimensions (L x W x H)	1.5 m x 1.1 m x 1.9 m
Total Weight*	∼50 kg
Available Payload*	∼50 kg
Drive Mode	Two trolling motors (Differential drive)
Max Speed	1.5 m s^{-1}
On-board sensors	3D LiDAR, MBES, Cameras, GPS, IMU
Power Supply	3S rechargeable LiPo batteries
Operation Time*	∼2 h
Operation Time (Full config)**	∼1.5 h
Beaufort Scale***	Wind State: 2 (up to 11 km h^{-1}) Sea State: 3 (up to 0.6 m)

* Values acquired using the minimal configuration, energy and navigation modules only.
** Values acquired using the full configuration, energy, navigation, perception, and localization modules.
*** Dependant on the type of pontoon.

The drive system is composed by two thrusters configured for differential drive at the stern of the vessel. It uses standard trolling motors with a maximum thrust around 250 N with a maximum power consumption of 360 W each. The motors are connected to a commercial brushed dc motor drive with dual-channel to receive commands from an on-board PC, while

[5]Encyclopedia Britannica, 2022. *Beaufort scale*. URL: https://www.britannica.com/science/Beaufort-scale

sending power inputs, using PWM control, to the motors. This allows the SENSE to reach speeds up to 1.5 m s^{-1} using the pontoons depicted in Figure 1. In this figure is presented the design of the SENSE in full configuration, composed by two thrusters, Wi-fi antenna, 3D LiDAR, stereoscopic camera, MBES, GPS and IMU.

FIGURE 1. The SENSE full configuration mount. Green, orange, blue and red squares are the energy, localization, perception and navigation modules, respectively.

B. HARDWARE ARCHITECTURE

The SENSE hardware architecture is subdivided in four modules, namely energy, navigation, perception and localization, as depicted in Figure 2a. Each one of them is built in a single watertight enclosure that is attached to the aluminum frame. The minimal configuration required for the ASV to be fully functional is constituted by the energy and navigation modules, which provides the required power and control systems for the vehicle to operate, as well as a remote Wi-fi access point. The addition of the other modules, perception and localization, enhances the vessel potential beyond the navigation ability by introducing the capacity to acquire and process perception data and improving the localization and navigation sensors accuracy. This modularity yields the advantage of allowing a straightforward modification of single modules independently, without requiring a major re-engineering effort to the vehicle itself. Moreover, its important that the weight of the modules is distributed along the rigid frame to ensure that the centre of mass is near the middle of the vehicle, thus avoiding any unevenness that can compromise the vehicle safety and stability.

The energy module is responsible for providing power to all available modules and is composed by the battery and the power distribution systems. As illustrated in Figure 2a, it is linked to all the modules available in the system and is composed by several lithium batteries in parallel with a total capacity of 555 Wh. Currently, it uses ten 3S LiPo batteries with 5000 mAh each. This payload offers an autonomy around 2 h for the minimal configuration. This operation time is dependent on the modules in use, their composition and the installed pontoons. Nevertheless, the vehicle endurance can be enhanced with higher capacity sources, different technologies (e.g. supports 4S LiPo batteries), or by adding more batteries to the module. Moreover, the energy module can easily be replaced by a similar assembly during the mission.

The navigation module provides the motor drive controller and allows the remote or autonomous operation of the SENSE, while serving as the communication relay with a remote ground station. This enclosure is composed by a power supply unit (PSU), an embedded computer, the navigation sensors (GPS and IMU) and the motor drive. The PSU regulates the power for all the components and protects the system from undervoltage and overvoltage states. It also provides an emergency switch option that cuts-off the motor power while maintaining all processing capabilities. An embedded computer (Odroid XU4) is used to send commands to the motor drive, to interact with the radio controlled (RC) transmitter for remote operation and to create a local network to interface with the other modules. Additionally, the Odroid creates a Wi-fi network that broadcasts the vehicle information to a remote location, namely a ground station. The on-board GPS and IMU sensors are connected to the embedded computer for their acquisition and processing, and can be used for the autonomous navigation if no other solution is available. Moreover, the computer can be used to execute more advanced features, such as waypoint navigation, collision avoidance and geopositioning.

As for the perception module, the PSU outputs the power for the computer and regulates the voltage to 5 V, 12 V and 24 V, which then can be used to power the available sensors on the selected payload. The embedded computer employs a mini-itx motherboard solution equipped with an Intel i5-8400@2.80 GHz CPU, a 16 GB RAM and 1 TB SSD storage, as well as ethernet and USB 3.0 communications. This provides a platform with higher computational capacities to acquire, process and store sensor data to be used during real-time operation or to be analyzed offline.

The localization module provides extra navigation sensors and an Odroid XU4 to read the data and estimate the localization of the vehicle. This adds redundancy to the ASV positioning system with high-end GPS and IMU sensors, that allows a more accurate localization estimation with access to new technologies, for instance real-time kinematics (RTK), which can be used as ground-truth due to its centimetrical precision.

The addition of new modules besides the ones presented here can be achieved by connecting the new box to the local network and to the energy module. For instance, it can

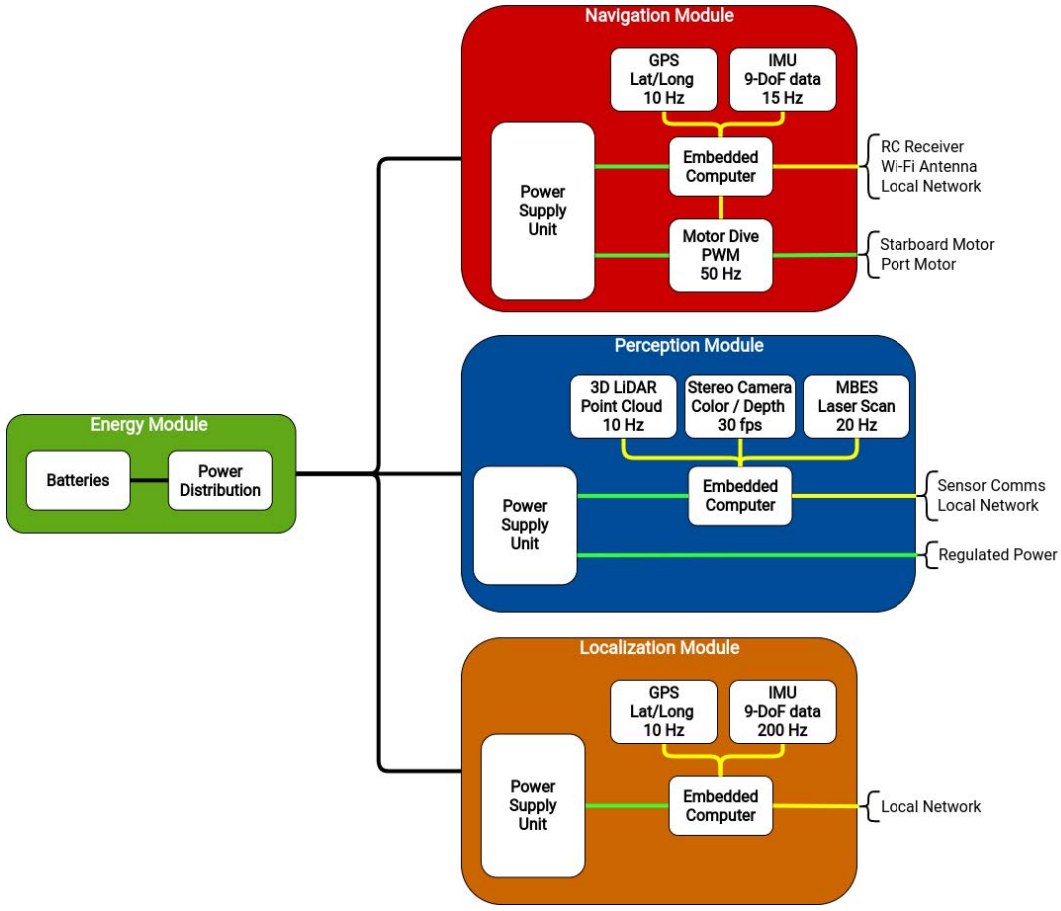

(a) Hardware architecture. Yellow, green and black lines are the communications, regulated power and energy supply connections, respectively.

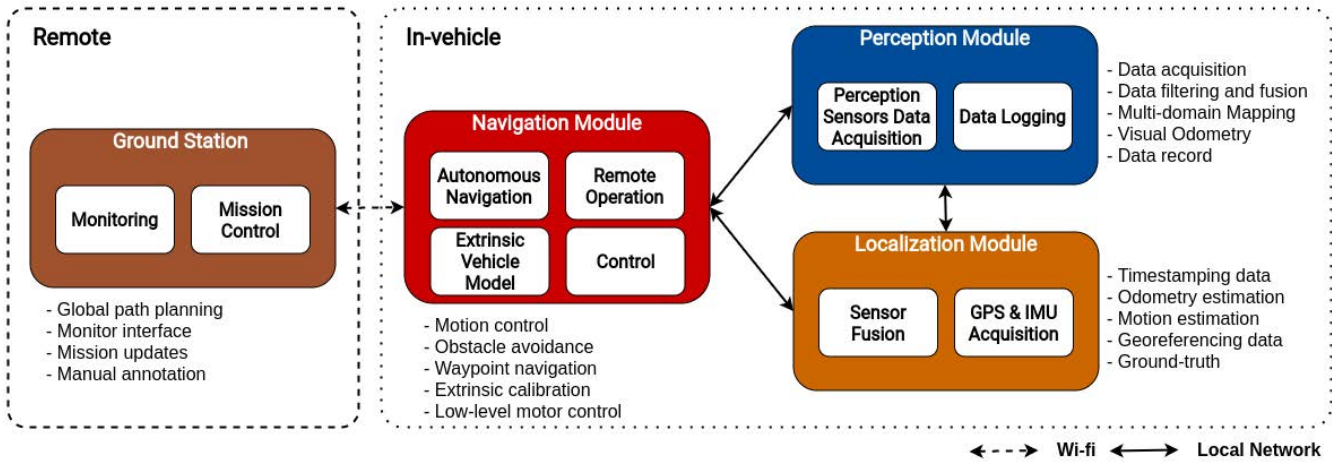

(b) Software architecture.

FIGURE 2. **SENSE hardware and software architecture.**

be added a communication relay module for the interaction with underwater vehicles. Figure 1 depicts the complete configuration of SENSE, where the green, orange, blue and red squares are the energy, localization, perception and navigation modules, respectively.

C. SENSOR PAYLOAD

The observation of multi-domain scenarios demands the use of heterogeneous sensors capable of fulfill the distinct requirements for each domain, namely the surface and underwater regions in the maritime scenario. Thus, a setup that

includes sensors capable of operating in each one of the domains is vital to increase observability of the vehicle while allowing to pinpoint the geolocalization of the data. This setup includes the use of different sensors organized in a cost-effective resource.

The navigation and perception sensors,[6] as well as their placement in the SENSE are presented on the next subsections.

1) NAVIGATION SENSORS

The navigation sensors available in SENSE are distributed between the navigation and localization modules. The used sensors are:

- Sparkfun Razor IMU 9DOF, 15 Hz, 9 axis, 1.0°/2.0° angular accuracy. This is available in the navigation module and is a low-cost IMU solution presenting a lower accuracy;
- Xsens MTi-30 IMU, 200 Hz, 9 axis, 0.2°/0.5° angular accuracy. This is available in the localization module and is a high-end IMU solution with high accuracy;
- Vk-162 Glonass GPS, up to 10 Hz, GNSS, 2.0m horizontal accuracy. This is available in the navigation module and is a low-cost GPS solution with lower accuracy, more susceptible to signal loss and noisy measurements. No external antenna is available;
- Swift Navigation Piksi Multi GPS, up to 10 Hz, L1/L2 RTK, 0.01m horizontal accuracy and 0.015m vertical accuracy. This is available in the localization module and is a high-end GPS solution with higher accuracy and with a more stable signal. This sensor when paired with a base station also provides a L1/L2 RTK technology with an Euclidean error lower than 0.05 m that provides the ground-truth for localization based methods.

2) PERCEPTION SENSORS

The perception sensors available in SENSE are connected to the perception module. The used sensors are:

- Imagenex "Delta T" 837B. Multibeam Echosounder with a rate up to 20 Hz, 120 beams, able to acquire data from a minimum range of 0.5 m to as far as 100 m, maximum distance. Resolution of 0.2% of the range;
- Mynt Eye D. Stereo camera with a rate up to 60 fps, and a maximum resolution of 1280 × 720;
- Velodyne VLP-16. LiDAR with a rate of 10 Hz, capable of measuring distance up to 100 m and field of view of 360° horizontal and 30° vertical. Accuracy of 0.03 m.

3) SENSOR DISPLACEMENT

The sensor payload and setup installed in SENSE to acquire the dataset is depicted in Figure 3, as well as the coordinate frames for their physical placement, where the red, green and blue lines represent the *X*, *Y* and *Z* axis, respectively. In Table 3 the relation between the sensors and the coordinate frames in Figure 3 are listed, as well as the position in meters from each in relation to *base_link*.

TABLE 3. Sensors available in SENSE, respective frames and position in meters from Figure 3.

Sensor	Frame	Position (x,y,z) m
Sparkfun Razor IMU 9DOF	imu_nav_box	(0.48,-0.17,0.09)
Xsens MTi-30	imu	(0.98,0.17,0.09)
Vk-162 Glonass GPS	ublox_gps	(0.27,-0.20,0.12)
Swift Navigation Piksi Multi	gps	(0.80,0.10,1.09)
Velodyne VLP-16	velodyne	(0.93,0.0,0.70)
Mynt Eye D	mynteye_left_color_frame mynteye_right_color_frame	(0.99,0.07,0.68)
Imagenex "Delta T" 837B	sonar_link	(0.45,0.0,-0.50)

D. SOFTWARE ARCHITECTURE

A public repository from INESC TECs' CRAS is available at https://github.com/danielfbcampos/SENSE.git. The repo provides an open-source example of the software available on the SENSE. The on-board software architecture defines the autonomous navigation and remote-operation methodologies, as well as the middleware used to communicate with the sensors. The system uses ROS (Robot Operating System)[7] with a hybrid communication network configuration, where the local network is distributed through gigabit Ethernet switches that links all nodes between modules, and the remote access uses a centralized configuration, available through a Wi-fi connection, Figure 4. To ensure robustness to updates, the ROS packages and tools used are the most widely integrated and stable, to minimize the impact on the software, since they are the less prone to suffer changes and the adaptations are easily applied. Moreover, the data buffering and timestamping provided by ROS allows to minimize the impact of packet loss, where all timestamps are synchronized with the master module using a Network Time Protocol (NTP) designed to perform well with intermittent network connections, and heavily congested networks, having a sub-microsecond accuracy. Moreover, to ensure the mission safety, the navigation module is used to create the ROS master, that tracks all publishers, subscribers and parameters. Thus, in case of a system failure on any other module it is always possible to control the ASV. In the event of a navigation failure, the mission is aborted and the thrusters are halted. As depicted in Figure 2b, a remote ground station, currently a laptop with Wi-fi conectivity, can be used to transmit new missions for the vehicle, to monitor the current state and to read the sensor data, such as images and point clouds.

[6]The sensors specifications are available on the vendors' datasheets.

[7]ROS, 2020. *Robot Operating System*. URL:https://www.ros.org/

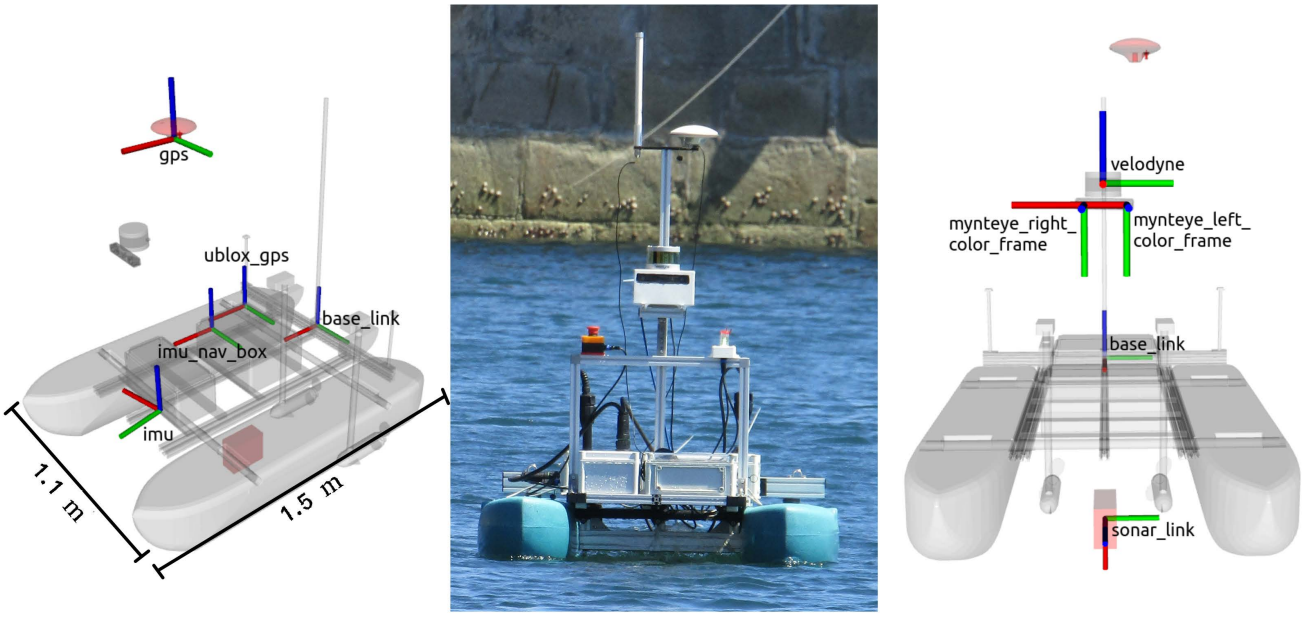

FIGURE 3. Setup of sensors used on the SENSE. The navigation sensors coordinate systems (left), the SENSE (centre) and the perception sensors coordinate systems (right). The red, green and blue lines represent the *X*, *Y* and *Z* axis, respectively.

The mission message is composed by a set of waypoints as well as the tasks to perform, for instance the vehicle can capture specific data in a position, passthrough or return home.

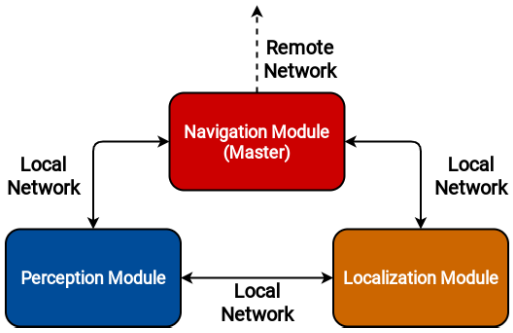

FIGURE 4. Communication network on SENSE.

The function for each in-vehicle modules are:

- Navigation module - controls the vehicle motion by providing commands to the motor drive received from either remote or autonomous navigation systems;
- Perception module - acquires and processes all sensor data and logs the topics from all modules into a solid-state drive (SSD);
- Localization module - receives GPS and IMU data and uses sensor fusion methodologies to estimate the SENSE position and orientation.

In Figure 5 is depicted the control scheme where the red, orange and blue nodes are executed on the navigation, localization and perception modules, respectively. This control receives a mission plan from a file or a ground station and the mission execution manages the current goal to visit with regard to the current pose. Then, the GoTo estimates the velocity required to reach the waypoint, which passes through a velocity selector that verifies if no safety measure is activated or if there is a remote operation bypass. At last, the velocity selector sends the command velocities v_c (linear) and ω_c (angular) to be converted to the motor commands.

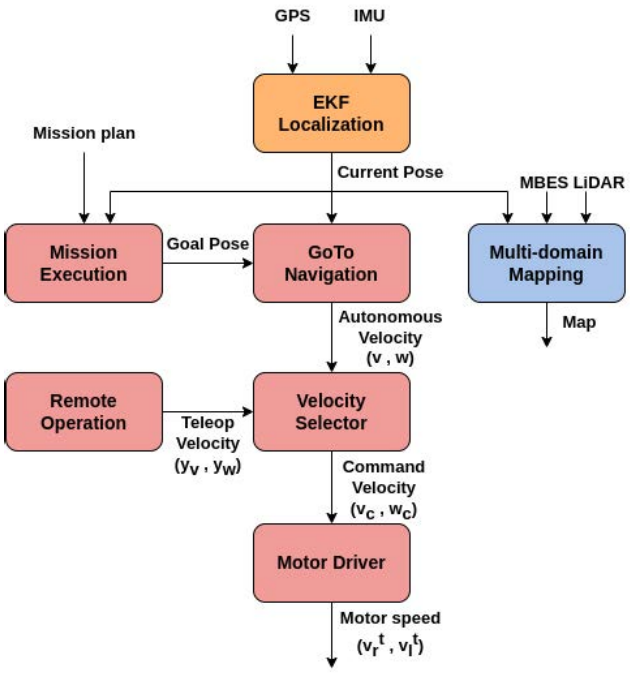

FIGURE 5. Control diagram for the operation of SENSE.

1) NAVIGATION MODULE

The navigation module controls the vehicle motion either on remote or autonomous operation. Each mode provides linear and angular velocities for the SENSE and at the low level control software a prioritization is made, where the remote commands have higher priority than the autonomous mode. This allows an on-mission mode switching, which increases the flexibility and safety of the vehicle by allowing to halt the mission and pass the control for a trained pilot, for instance in case of a system failure or if a new goal outside the mission scope is required.

The final linear and angular velocities are then converted to the velocity per thruster required for the ASV to reach that velocities. As such, a differential drive kinematic model is applied, where the speeds v_r^t and v_l^t affected to each thruster can be determined from equations (1) and (2), where α and β are constants for thrusters placement and configuration within the ASV, v is the linear velocity and ω the angular velocity [7]. Currently, the thruster control is made through the Roboteq driver in open-loop control since the used thrusters does not provide any feedback.

$$v_r^t = \alpha \cdot v + \beta \cdot \omega \tag{1}$$

$$v_l^t = \alpha \cdot v - \beta \cdot \omega \tag{2}$$

For the remote operation, a 2.4 GHz RC transmitter is used to alternate to tele-operated mode and to send the velocity commands. The controller joystick states are mapped to the linear and angular velocities by using the linear regression presented in equation (3), where y is the velocity (linear, y_v, or angular, y_w), s is the stick scale and the subscripts *min* and *max* defines the minimum and maximum values for the velocity and the scale. This transmitter also allows to override all autonomous navigation commands or to activate a safety procedure that halts the ASV motion during emergency situations.

$$y = \frac{(y_{max} - y_{min}) \cdot (s - s_{max})}{s_{max} - s_{min}} + y_{max} \tag{3}$$

As for the autonomous navigation, it uses the estimation from the localization module or assesses itself by fusing the in-module GPS and IMU data to estimate the pose. This 6DOF localization is obtained through the fusion of both sensors using an Extended Kalman Filter (EKF) as described by Campos et al. [8]. In this filter, the prediction model used to project the system state forward in time is based on a 3D kinematic model derived from Newtonian mechanics, with a 12-dimensional state vector composed by the vehicle 3D pose, orientation, and their respective velocities. The EKF predicts the SENSE poses throughout time when no sensor measure exists by using this omnidirectional motion model. When a new sensor reading is perceived the estimate is corrected. To support distinct sensors, it is assumed that each sensor produces measures of the estimated state variables, thus the H observation matrix is an identity matrix. Nevertheless, the sensors are asynchronous and do not measure all state vector variables independently, partial updates of the state vector are performed. This is achieved by reducing the observation matrix H to a m by 12 matrix with the only nonzero values (in this case set to 1) being the m measured variables [46]. The EKF filter inputs are the IMU attitude (roll, pitch and yaw) and angular velocity data, and the positional information of an odometry inferred from the GPS and IMU initial state. The latter is acquired by projecting the GPS data to the Universal Transverse Mercator (UTM) using the transformation defined in the USGS Bulletin 1532 [47] given by the Equations (4) and (5), where k_0 is the scale on central meridian for UTM, e the first eccentricity and ϕ the latitude in radians.

$$x = k_0 \cdot N \cdot \left(A + \frac{(1 - T + C) \cdot A^3}{6} + \frac{5 - 18T + T^2 + 72C - 58e'^2}{120} \right) \tag{4}$$

$$y = k_0 \cdot \left[M - M_0 + N \cdot tan\phi \cdot \left(\frac{A^2}{2} + \frac{(5 - T + 9C + 4C^2) \cdot A^4}{24} + \frac{(61 - 58T + T^2 + 600C - 330e'^2) \cdot A^6}{720} \right) \right] \tag{5}$$

The auxiliary variables, e'^2, N, T, C, and A are defined on equations (6) to (10), where a is the semi-major axis for WGS84, λ is the longitude in radians and λ_0 the origin longitude for the current UTM zone. M is the true distance along the central meridian from the Equator to ϕ obtained from equation (11) and $M_0 = M$ calculated for ϕ_0, the latitude crossing the central meridian λ_0,at the origin of the x, y coordinates.

$$e'^2 = \frac{e^2}{1 - e^2} \tag{6}$$

$$N = \frac{a}{\sqrt{(1 - e^2 \cdot sin^2\phi)}} \tag{7}$$

$$T = tan^2\phi \tag{8}$$

$$C = e'^2 \cdot cos^2\phi \tag{9}$$

$$A = cos\phi \cdot (\lambda - \lambda_0) \tag{10}$$

$$M = a \cdot [(1 - e'^2/4 - 3e'^4/64 - 5e'^6/256) * \phi - (3e'^2/8 + 3e'^4/32 + 45e'^6/1024) \cdot sin(2\phi) + (15e'^4/256 + 45e'^6/1024) \cdot sin(4\phi) - (35e'^6/3072) \cdot sin(6\phi)] \tag{11}$$

With the UTM projection the odometry is estimated from the position evolution throughout time in relation to the first GPS coordinate acquired and the correspondent initial rotation from the IMU.

Moreover, from the current pose and the mission waypoints list the next task to perform is selected. For such, a waypoint navigation (GoTo) is performed to sequentially visit the goals, evaluating the ASV heading error and the euclidean distance through the architecture depicted in Figure 6.

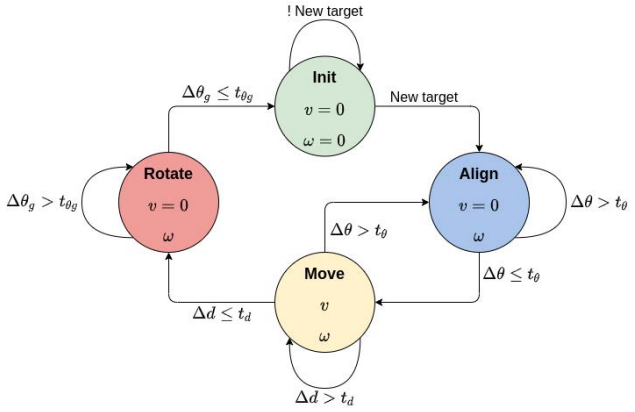

FIGURE 6. Waypoint navigation architecture.

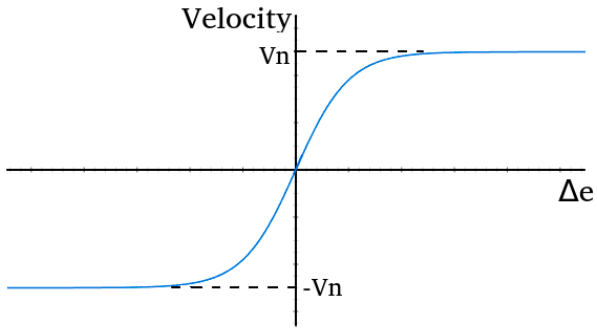

FIGURE 7. Hyperbolic tangent function example.

While no target arrives the ASV remains stationary with no linear and angular velocity, v and ω, respectively. When the mission starts, the vehicle rotates to align with the waypoint direction until a predetermined threshold, t_θ, is achieved. At this stage, the linear velocity is zero and it estimates the angular velocity through the equation (12), where $\Delta\theta$ is the angular error from the ASV heading to the waypoint direction angle, normalized between $-\pi$ and π, k_w is a smoothing gain and ω_n the nominal angular velocity.

$$\omega = tanh(\Delta\theta \cdot k_\omega) * \omega_n \tag{12}$$

With the ASV fairly aligned, the waypoint navigation enters the move state. It estimates the angular velocity similarly to the previous stage to perform small direction adjustments and the linear velocity is estimated by equation (13), where Δd is the distance to the waypoint, k_v is a smoothing gain and v_n is the nominal linear velocity. If a major misalignment with the target direction is detected, the vehicle reenters the align state.

$$v = tanh(\Delta d \cdot k_v) * v_n \tag{13}$$

The hyperbolic tangent function in equations (12) and (13) is used to smoothen the velocity required in order to minimize the error (Δe) towards the desired position while limiting the speed to the nominal velocity (V_n) when the error tends to infinity, as depicted in Figure 7.

When the distance to the waypoint is under the predefined threshold t_d, the ASV is oriented to the final heading. It uses a similar approach to the align state providing only angular velocity with $\Delta\theta = \Delta\theta_g$, where $\Delta\theta_g$ is the angular error between the current attitude and the target desired angle. At last, the ASV is considered to be aligned with the objective once the angular error is bellow the threshold $t_{\theta g}$, thus proceeding to the next mission goal.

2) PERCEPTION MODULE

The perception module creates the interface with all installed sensors. It runs all middleware nodes required to acquire and publish the sensors information in real time, as well as to perform data filtering and processing methodologies. Due to the higher computational power available, this module will also execute the methodologies to increase the situational awareness of the vehicle. Thus, this module will be endowed with the capability to perform highly demanding perception-based tasks, such as multi-domain mapping [8], detection of docks [48], vessel detection and tracking [49], and obstacle detection [50].

This module also provides 1 TB storage to hold and log the data from all vehicle systems using ROS bags. Depending on the information required for the mission being executed and the selected topics the log size may vary. This data can be physically retrieved from the disk or perform the copy through SSH onshore via Wi-fi to avoid compromising the bandwidth and decrease the data quality.

An example of the data gathered by the perception module with the corresponding sensor alignment in the SENSE is depicted in Figure 8. This provides one example of the data obtained by the available perception sensor payload, namely a pair of images from the stereo camera, the LiDAR point cloud and the MBES scan (line under SENSE).

3) LOCALIZATION MODULE

In the localization module the absolute position is estimated with the GPS, and the linear acceleration, angular velocity and orientation of the ASV is obtained from the IMU sensor. The data acquired from this sensors are fused to estimate a 6DOF pose using the EKF method previously described in the navigation module. The Swift Navigation GPS receiver used in this module also provides odometry estimations with centimetric precision using RTK technology. This technology uses a fix base station that sends differential GPS corrections to the rover (SENSE) via a dedicated wireless communication.

IV. RESULTS AND DISCUSSION

The heterogeneous payload available on the SENSE provides information of the vehicle state and of both domains in the maritime environment, namely surface and underwater. As such, distinct modalities, information, rates and noise affect the available data.

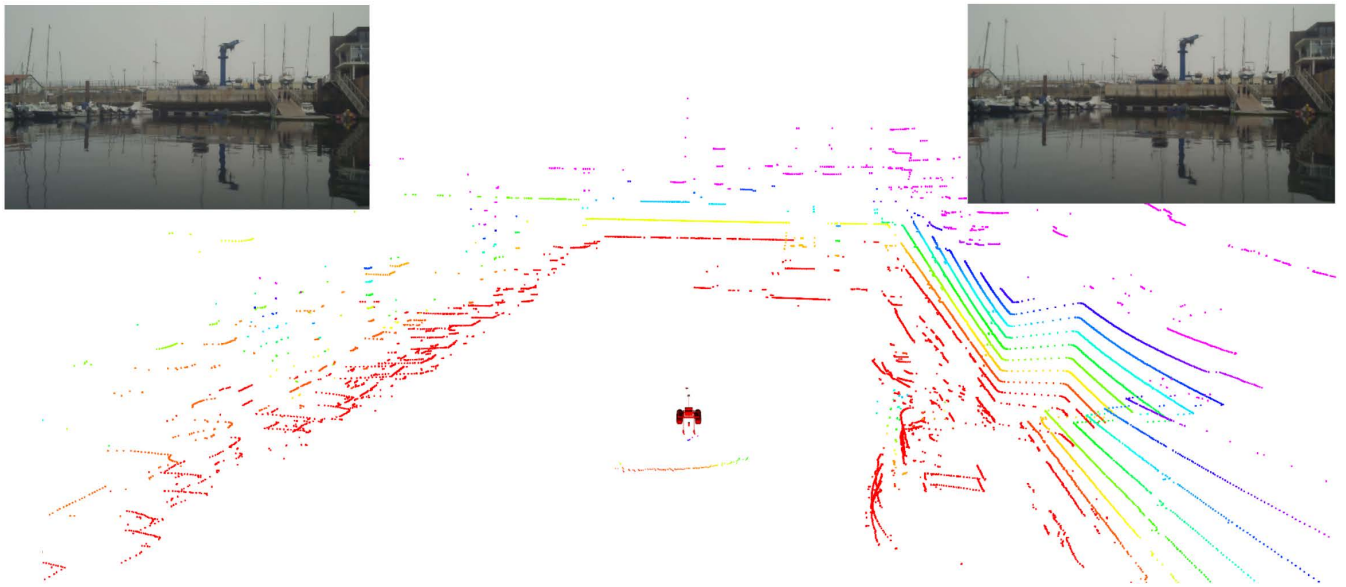

FIGURE 8. The 3D representation of a SENSE aquired frame, based on data from the LiDAR and Sonar sensors. Stereoscopic images are presented on top.

Two field tests were performed with SENSE on the biggest port for yachting on the North of Portugal, namely the *Marina de Leça* harbor depicted in Figure 9. It has 240 mooring places available on site and has a depth of 4 m at the entry basin and 2-3.5 m at the yacht basin.[8] On the first test the minimal configuration was validated and on the second the full architecture was used. With the minimal configuration no data was collected only the navigation was tested, while part of the second test resulted on the data collection displayed on the ROAM@CRAS dataset.

Images of the two field tests performed with SENSE and a preview of the dataset can be found in the video available on: https://youtu.be/vkJ-MVCSpdA. All the presented data on this section were retrieved from the ROAM@CRAS dataset.

A. ROAM@CRAS DATASET

The ROAM@CRAS is ROS-compliant and all sensor data collected from scenarios is stored in bag files. ROS is a well adopted technology, mainly in the fields of mobile and industrial robotics, and preserves the output rate of sensors, saves the timestamp of the data and describes the extrinsic relations between sensors, being ready to use online and offline. A public repository from INESC TECs' CRAS with the dataset is available at https://rdm.inesctec.pt/dataset/nis-2020-002 [51].

The ROAM@CRAS presents the result of a mission performed during the field tests of SENSE at the harbor with the full modules and sensor payload presented in Section III. A tele-operated route is performed on this harbor and provides data obtained by several sensors allowing the acquisition of navigation information through GPS and IMU from the localization module, plus perception data of the two domains with a 3D LiDAR and a stereo camera (surface) and a multibeam echosounder, MBES (underwater).

This dataset was acquired on a partially cloudy day, Figure 9b, with slow wind speeds (4km/h North) and good illumination circumstances. As depicted in Figure 9a from Google Maps,[9] the test site presents heterogeneous scenarios with several dock types (e.g. U-Shaped and I-Shaped), static features (e.g. bridge columns), dynamic features (e.g. docks with distinct vessels and states), open areas with few features and various depth conditions. The dataset provides a comprehensive ensemble of conditions that illustrates a realistic set of typical events on a fully functional harbor namely:

- The SENSE docking and undocking;
- Crossings with other vessels;
- Observation of distinct types of docks and vessels;
- Perception of the two dock states, occupied and free.

1) DATA COLLECTION METHODOLOGY

The data collection was acquired through the remote operation by a trained driver on board of a crewed support vessel. It reached velocities up to 1.2 m s^{-1} and stored the data from all on-board sensors and some internal states of the vehicle.

The operation time span was roughly 20 min (∼1196 s) stored in multiple 14 s patches. The mission starts with the ASV moored for a few seconds then it launches through the canal. The SENSE observes distinct harbor features, namely multiple types of docks, mainly U-shaped and I-shaped, with occupation states that changes throughout time, several vessels either berthed or moving, and fixed structures, such as the bridge with column foundations at the southeast side and the

[8]Marina Porto Atlântico, 2020. *Marina Porto Atlântico*. URL: https://www.marinaportoatlantico.net/en.

[9]Google Maps, 2020. *Marina de Leça*. URL: https://goo.gl/maps/CAXmn8Qg921EUJKs6.

(a) Satellite view (41°11'13.8"N 8°42'18.3"W)

(b) Dataset acquisition conditions.

FIGURE 9. ***Marina de Leça*** **harbor - 240 mooring places with entry and yacht basins depth of 4 m and 2-3.5 m, respectively.**

breakwater surrounding the harbor. At the end, the SENSE returned to the initial docking area. The trajectory performed by the SENSE during the acquisition of the ROAM@CRAS dataset is depicted in Figure 10, where the green line is the RTK observations and the red arrow points to the base station position on the harbor.[10]

FIGURE 10. **Trajectory performed by the SENSE on** ***Marina de Leça*****. The green line is the RTK observations and the red arrow points to the base station position[10].**

Along the route distinct situations are covered trying to maximize the generalization of common challenges on harbor scenarios and to test the observability limitations, namely:

- The SENSE presents variable velocities from halt periods, to ensure the safety in intersection situations, to faster velocities;
- Crossings with other vessels operating in the harbor, that results on halt situations;
- Steeper waves caused by larger vehicles in transit;
- Temporary data occlusion by dynamic elements;
- Navigation in close range to metallic structures with the possibility of noisier sensor estimations by the navigation sensors;
- Acquisition of close-range data with more detailed measurements from the perception sensors;
- Limited the MBES field-of-view range to 5 m to create data incompleteness situations. For instance, at the entry basin few or even no observations are made in multiple scans.

Thus, a comprehensive set of occurrences are illustrated throughout the full operation, that provides several challenges for applications, such as mapping, feature extraction, structure classification and obstacle detection.

The data gathered from all the sensors on SENSE are available in the ROAM@CRAS dataset and can be subscribed through the ROS topics listed on Table 4, where *VK-GPS* is the Vk-162 GPS, *SN-GPS* is the Swift Navigation GPS, *R9-IMU* is the Razor 9DOF IMU and *XS-IMU* is the Xsens IMU.

2) SENSOR CALIBRATION AND SYNCHRONIZATION

The sensor payload extrinsic calibration and synchronization was represented using ROS available tools for transform and timestamp the data. The localization module sensors, the Velodyne and the Mynt Eye were calibrate and synchronized following the same procedures as in a previous work by Gaspar et al. [30] for acquiring a dataset on an urban scenario.

The extrinsic calibrations for all sensors are available on the dataset repository (https://github.com/danielfbcampos/ROAM-CRAS). It represents the physical displacements and orientations of each sensor in relation to the coordinate system of the base frame, previously presented in Figure 3.

[10]Base station positioned on the coordinates 41° 11'13.7"N 8° 42'18.4"W.

TABLE 4. List of the data available in the ROAM@CRAS and the respective ROS topics.

Sensor	ROS topic	Summary
Internal	/cmd_vel /left/cmd /right/cmd /roboteq_driver/status /safety_stop	- Velocity commands - Thruster commands - Vehicle diagnostics
R9-IMU	/imu_nav/data	- Angular velocity - Linear acceleration - Orientation
XS-IMU	/imu/data /velocity	- Angular velocity - Linear acceleration - Orientation
VK-GPS	/ublox_nav/fix /ublox_nav/fix_velocity	- Latitude - Longitude - Altitude - Linear velocity
SN-GPS	/gps/fix /gps/rtkfix /gps/time /gps/basestation_ecef	- Latitude - Longitude - Altitude - Odometry - Linear velocity - Time reference - Base station location
LiDAR	/velodyne_points	- 3D points
Camera*	/depth/camera_info /depth/image_raw /left/image_color** /right/image_color**	- Depth - Compressed Raw Images - Calibration
MBES	/mbes/scan	- 2D Scan - Polar data

* All camera topics includes the prefix */mynteye*, e.g. */mynteye/depth/camera_info*.
** Compressed images, includes suffix */compressed*, e.g. */mynteye/left/image_color/compressed*.

The stereoscopic system, Mynt Eye D, was calibrated according to Wang et al. [52], using a chessboard to calculate the extrinsic parameters from corner extraction. The intrinsic parameters of the LiDAR are provided by the vendor.[11] To acquire the relation between the cameras and the LiDAR coordinate frames it was used the single value decomposition of a set of 3D correspondences from the work of Dhall et al. [53]. Finally, the IMUs and the GPSs frames were manually measured in relation to a reference coordinate system.

The synchronization of sensors can be verified through the timestamp information provided in the ROS messages. This timestamp returns the moment that data is acquired by the middleware for each of the installed sensors which presents asynchronous output rates.

3) DATA SAMPLES

a: NAVIGATION SENSORS

The navigation sensors available in the SENSE are composed by two GPSs (SN-GPS and VK-GPS) and two IMUs (XS-IMU and R9-IMU) that provide redundant data with distinct accuracies and rates.

The SN-GPS is used to acquire both RTK and GPS data. This sensor publishes the RTK data at a rate of 10 Hz with a centimetrical precision that can be used as ground-truth. As for the GPS data, the rate is approximately 8 Hz. Since both positional data are given by the same sensor, almost no difference is observed between the GPS and RTK measures, as depicted in Figure 11, where the GPS readings, blue line, overlaps with the ground-truth, green line (covered by the GPS trajectory). This overlap is also given by the scale factor since the error is within centimetrical precision, while the travel distance is approximately 620 m. As for the VK-162 GPS, the data is acquired at a rate of 4 Hz presenting a lower accuracy in comparison to the SN-GPS. As illustrated in Figure 12, where the green line is the ground-truth and the purple is the VK-GPS, the data presents major drifts in relation to the RTK. Since no external antenna is available for this sensor higher signal attenuation affects the data while being more susceptible to noise from the surrounding structures.

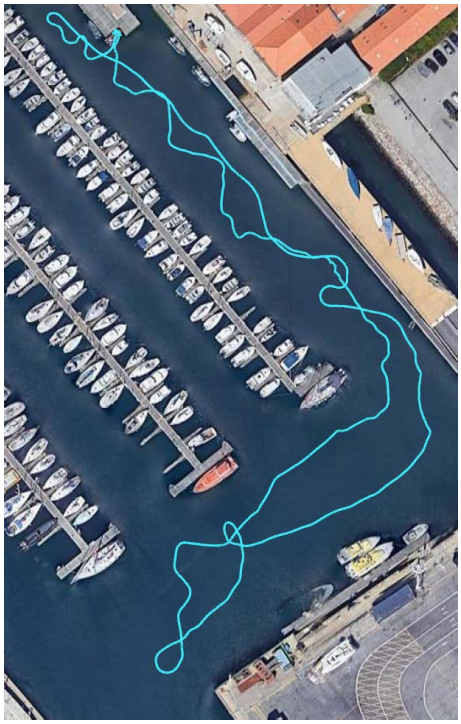

FIGURE 11. Swift Navigation GPS readings compared to the RTK ground-truth. The green and blue lines are the RTK and SN-GPS data, respectively. The error scale factor is minimal, thus the lines are overlapped.

The XS-IMU produces high frequency data at approximately 200 Hz with smooth orientation evolution through time and responsive angular velocities and linear accelerations readings. On the other end, the R9-IMU provides a lower rate, around 15 Hz with noisier orientation data and less sensitive angular velocities and linear accelerations.

Two distinct situations where selected to be illustrative of the qualitative difference of performance for both IMUs.

[11] VeloView-VLP-16-HiRes.xml on December 29, 2016

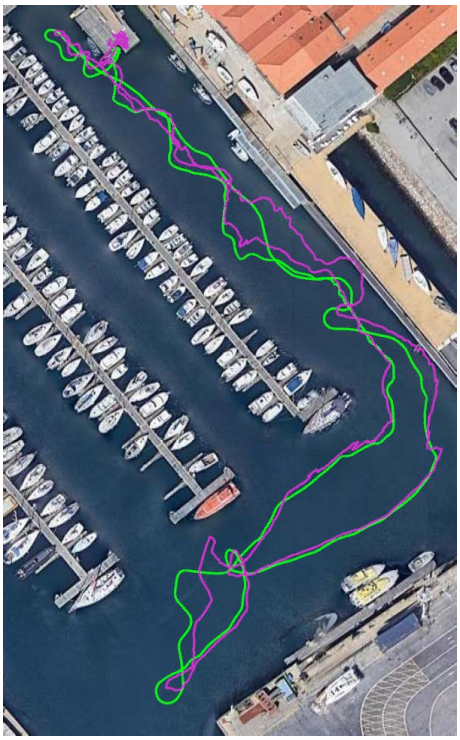

FIGURE 12. VK-162 GPS readings compared to the RTK ground-truth. The green and purple lines are the RTK and VK-GPS data, respectively.

In the first, the SENSE rotates in yaw with almost no linear velocity. In Figure 13 and Figure 14 are depicted the yaw, in degrees, and the corresponding angular velocity, in rad s^{-1}, acquired by both IMUs. The orientation given by the XS-IMU, green line, provides a smoother yaw evolution than the R9-IMU, red line. Thus, the Xsens is more in accordance with the vehicle kinematics, where large angular variations at small periods of time, such as the ones observed in the Razor IMU, are impossible. As for the angular velocity, given by the gyroscope of each IMU, it is possible to see a similar growth tendency for both, however they present a small deviation in the magnitude between them. Moreover, the Xsens IMU readings is able to detect smaller variations, since the acquisition rate is more then ten times quicker when compared to the Razor IMU, thus, being more responsive.

Lastly, at another instant, where the SENSE halts is movement and then resumes the mission, it is observed a distinctive variation on the vehicle linear acceleration around the *X* axis, which is aligned with the linear velocity vector given by the differential drive. Both IMUs are capable of detecting the variations, Figure 15, with the SENSE stopping around the first second and resuming the motion shortly after the eighth second. The data provided by both sensors fully depicts the two moments, nevertheless, such as in the angular velocity, the XS-IMU is capable of detecting more variations through time with less discretization of the acceleration. Moreover, the readings from the IMUs present a drift in the magnitude between each other.

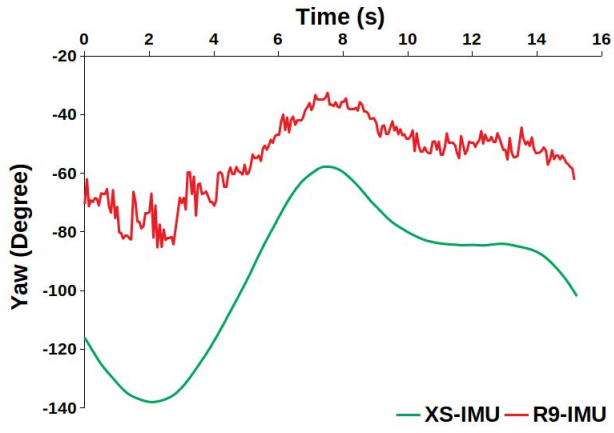

FIGURE 13. Yaw evolution through time.

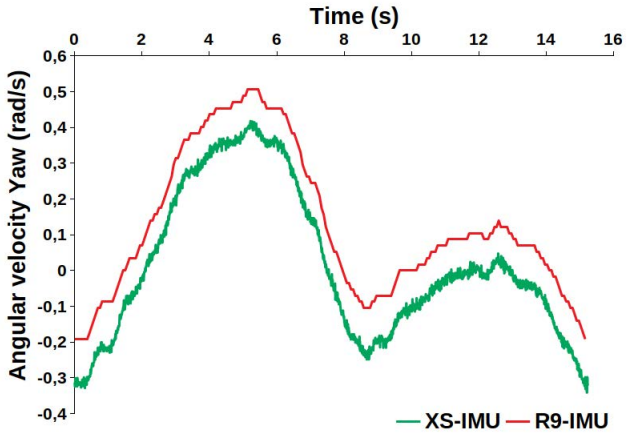

FIGURE 14. Yaw angular velocity evolution through time.

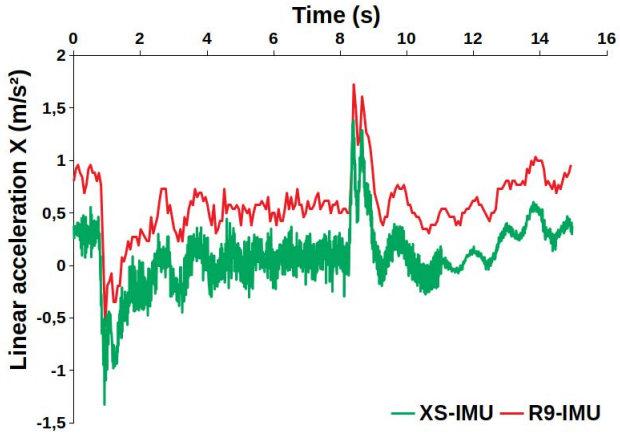

FIGURE 15. Linear acceleration in the *X* axis evolution through time.

b: PERCEPTION SENSORS

The ROAM@CRAS dataset offers an insight towards the data perceived by the SENSE on the harbor. To illustrate the data gathered by the perception sensors, namely the stereo camera,

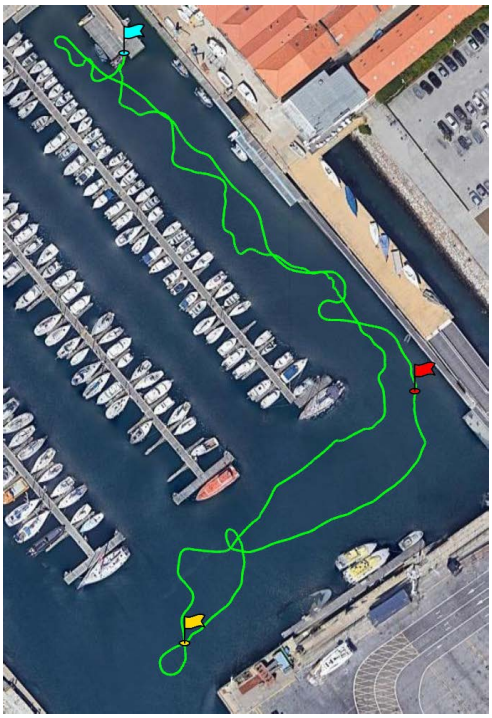

FIGURE 16. Locations of the example snapshots. Each flag corresponds to data acquisition instants.

(a) Left camera image.

(b) Right camera image.

FIGURE 17. SENSE stereo camera sensor, Mynt Eye D.

LiDAR and MBES, three snapshots were selected to highlight some scenario features. Figure 16 depicts the position for each one of them, where the flags with distinct color placed on the ground-truth trajectory represents the locations.

FIGURE 18. Camera data acquired in each location flagged in Figure 16.

The stereo camera system, Mynt Eye D, provides visual information from the scenario. The images retrieved by the Mynt Eye D have a resolution of

$$1280 \times 720$$

published with a rate of approximately 20 fps. Since the sensor has a short baseline, it generates a high overlap between the left and right cameras, as shown in Figure 17. As for the data collected throughout the mission, it portrays different challenges with both dynamic and static observations, during which the camera is affected by noise, varying lighting conditions and by the vehicle motion, causing motion blur.

In Figure 18 are depicted the images from the right camera retrieved on the locations flagged on Figure 16. At the first image, blue flag, the SENSE is docked. As it can be seen, there are several moored vessels and the yacht basin is clear. The second one, yellow flag, was gathered near the entry basin, where larger vehicles are moored and shipping containers from the Port of Leixões are on the line-of-sight. At last, the third frame, red flag, exhibits one static infrastructure available in the scenario, which can provide features that

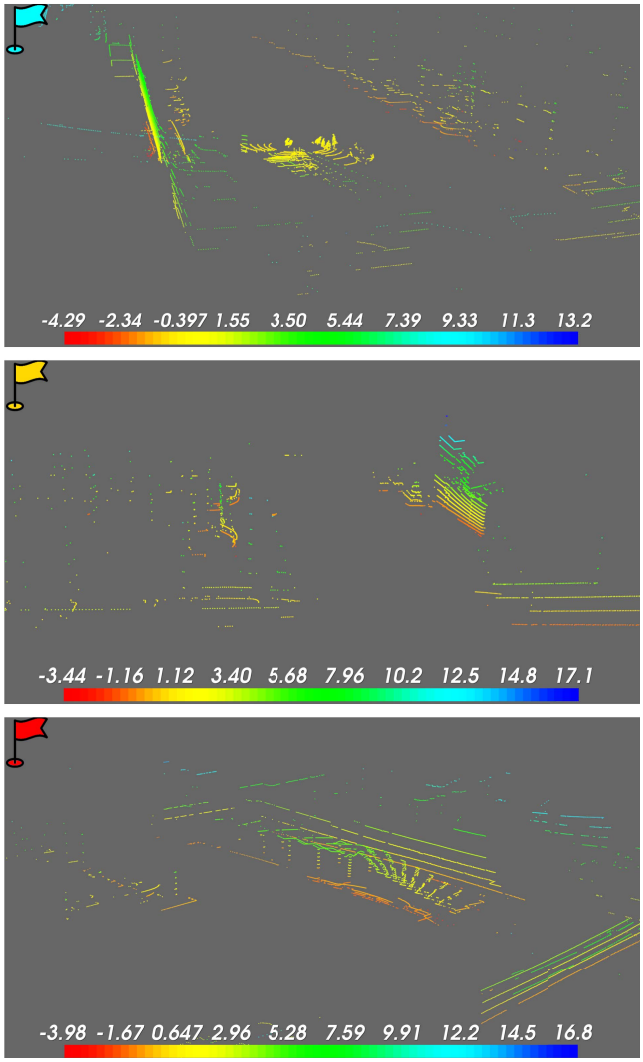

FIGURE 19. LiDAR data acquired in each location flagged in Figure 16. The scale illustrates the Z-axis (height) range in relation to the sensor.

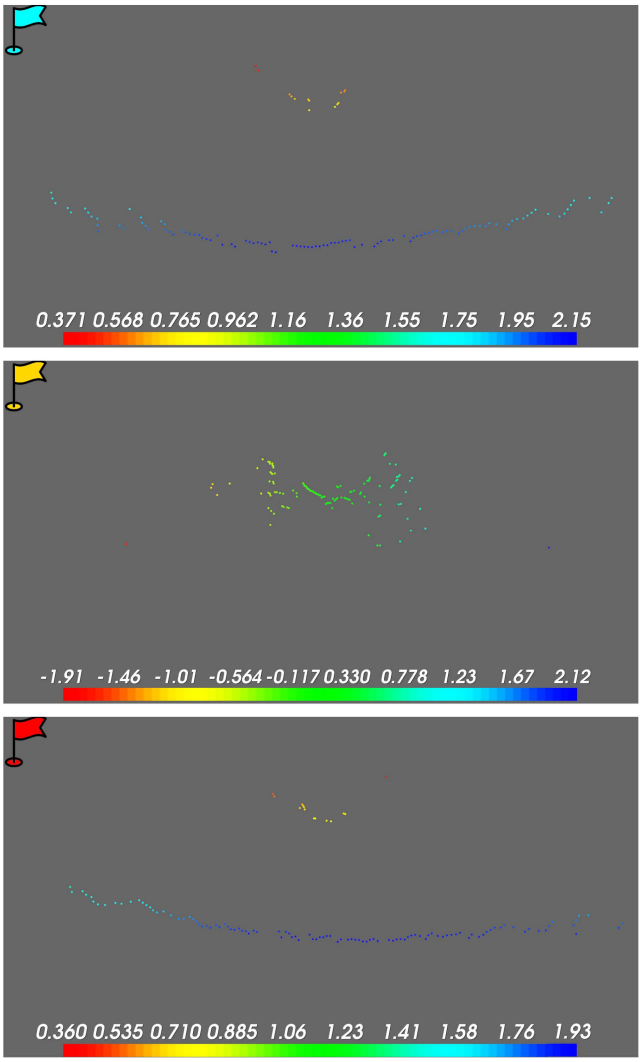

FIGURE 20. MBES data acquired in each location flagged in Figure 16. The scale illustrates the X-axis (depth) range in relation to the sensor.

can be used as feedback to test visual inspection techniques or other perception based methodologies, such as visual odometry.

Another available sensor is the LiDAR, Velodyne VLP-16, that provides 3D distance information of the surroundings with a frequency of 10 Hz and a range up to 120 m depending on the material reflectivity. It has a FoV of 330° horizontal, due to an occlusion resulting from the antennas mounting system, and 30° vertical. This sensor publishes high accuracy point clouds, where the higher the distances the sparser data becomes. Moreover, the sensor wave length is 905 nm, as such it can only penetrate 1 cm of the water surface providing no reflections, thus the wave impact will translate into missing data instead of spurious data [54].

In Figure 19 are depicted some examples of the surface point clouds from the SENSE. In the first snapshot it is possible to visualize the harbor facilities, such as piers, access ramps and stairs, several moored vessels, as well as people on the piers and on the support vessel. As seen, the data is denser near to the sensor itself, becoming sparser at further distances. This offers a challenge, since in some cases, when the SENSE navigates in wider areas, such as in the second snapshot, it will have less visible features to be used or even incomplete data. This is verified specially during operations in offshore locations where the scenarios are mostly open sea. For this, the use of a RADAR would be better to increase the field of view, mainly for bigger ships to detect objects earlier and increase the safety of the navigation. Nevertheless, during missions with several man-made structures that provide an elevated number of features, as well as constructions to inspect, the LiDAR provide accurate metric information for inspection purposes. The third snapshot is one example, where the bridge elements are visible, namely the pillars, the beams, the platform and the lower level piers. Also, throughout the dataset several docking spaces are depicted.

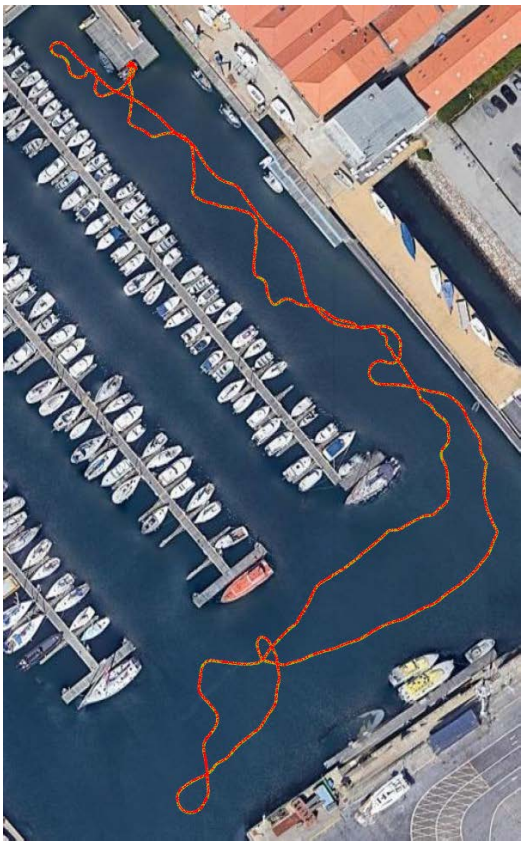

FIGURE 21. Odometry acquired through the GPS and IMU fusion. The green and red lines are the RTK observations and the GPS/IMU odometry, respectively.

At last, the available multibeam echosounder produces a 2D profile of the sea-bottom. The sensor is configured to publish data from 120 beams with a maximum range of 5 m at a rate of approximately 12 Hz. The selected beamforming method used on the Imagenex sensor detects the first echoes returned by each beam. Since the MBES is pointing downwards and the tidal waves were almost flat, the beams in the centre will correspond roughly to the depth of the seabed in relation to the sensor, which is placed 0.4 m bellow the water level.

The beamforming results at each snapshot location is illustrated in Figure 20. The first and last images captures the seabed near the yacht basin. The data acquired provides readings of 2.15 m and 1.93 m in each location to add up to the 0.4 m of the sensor placement below the water level, which is consistent with the information detailed by the harbor, where the yacht basin has a depth of about 2-3.5 m. As for the MBES scan in the yellow flag instant, the seabed depth is above the maximum range, where the available measurements are spurious measures given by erroneous reflections during beamforming. This will produce missing data during the SENSE passage through the entry basin, where the depth is higher than the expected 4 m.

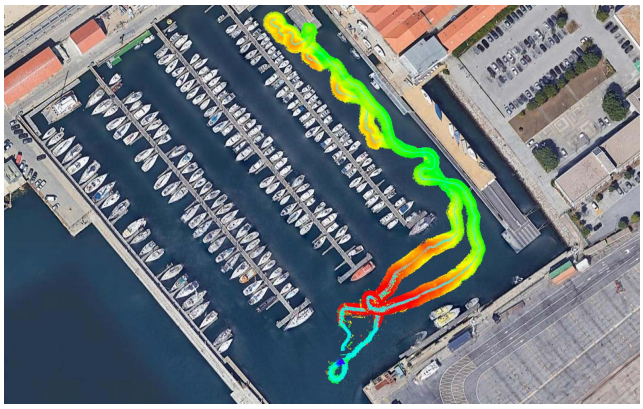

FIGURE 22. SENSE bathymetry acquisition. The rainbow presented goes from red (higher depths) to blue (lower depths). The green corresponds to intermediate values.

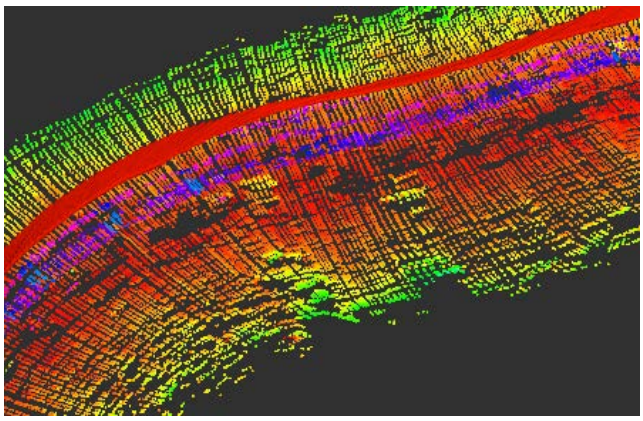

FIGURE 23. Close-up of the SENSE bathymetry.

B. APPLICATIONS

1) ODOMETRY ESTIMATION

Odometry provides useful navigational information that can be used to track the vehicle position evolution throughout time. It can be obtained from the navigation sensors, for instance using the method presented in the navigation module section, or from the perception sensors, namely the cameras and the LiDAR, e.g. the work proposed by Forster et al. [55],Teixeira et al. [56], Skjellaug et al. [57].

Since the SENSE is operating in areas with GPS availability the application of the GPS and IMU fusion method presented in the navigation module section provides an accurate odometry. As seen in Figure 21, it produces a similar trajectory to the available RTK ground-truth. Using the metric proposed by Zhang and Scaramuzza [58], this odometry estimation trajectory produces an average RMSE of 0.099 m and a standard deviation of 0.069 m for a travelled distance around 620 m.

2) BATHYMETRY

The data provided in the ROAM@CRAS dataset can also be used to develop and validate bathymetry methodologies.

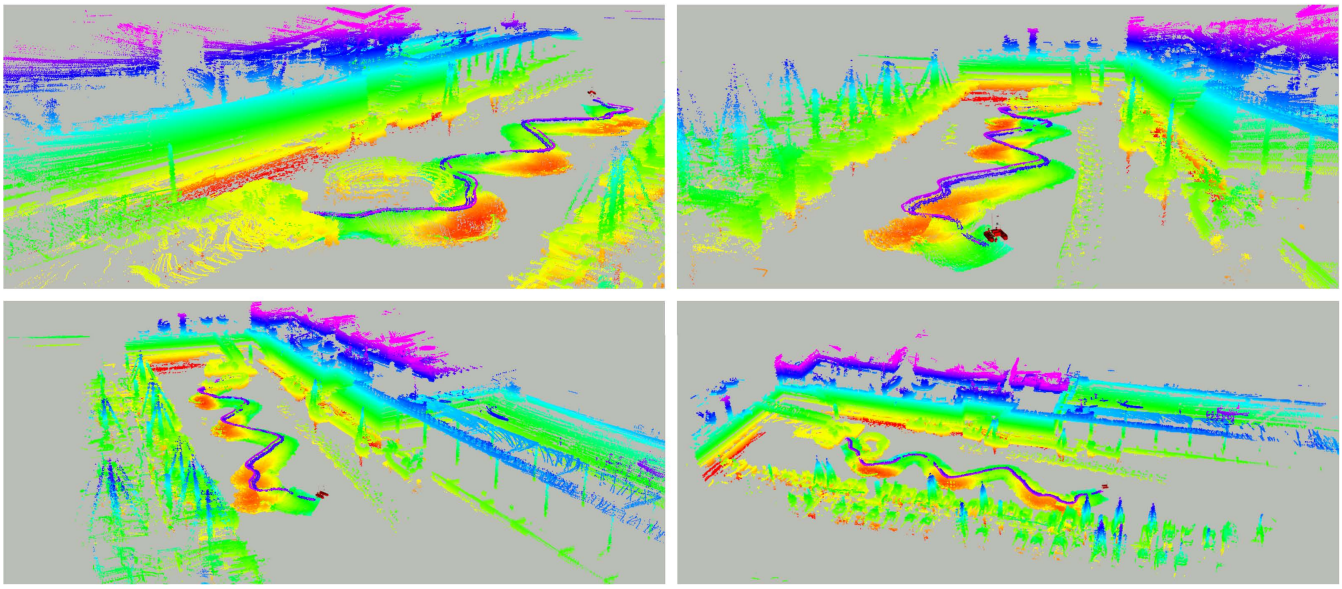

FIGURE 24. Multi-domain map on a partial sequence of the ROAM@CRAS. Retrieved from [54].

This can be applied to evaluate and explore the underwater domain. Moreover, it provides crucial information for infrastructure inspections, namely for representing the scour condition on offshore wind turbines or bridges foundations, and for depth estimation.

As an example, a simple bathymetry given by the association between the GPS and IMU odometry, acquired from the localization module, and the MBES scans without any filter is shown in Figure 22. This georeferenced MBES profiles were concatenated through time. In the performed trajectory it is possible to observe the depth increase as SENSE approaches the entry basin, where the data becomes unavailable, only noise readings were concatenated.

In Figure 23 a close-up of the bathymetry is depicted, where the seabed is concave with the deepest part in the centre of the observed route. Moreover, some artifacts are visible, for instance the isolated green measures on the red plane, which can be stones placed on the ground or the accumulation of sediments due to the currents.

3) MULTI-DOMAIN MAPPING

The creation of multi-domain representations of the maritime environment can increase the situational awareness for ASVs by depicting both the surface and underwater regions on a single map. This provides enhanced information for multiple purposes, such as:

- increase navigation safety, e.g. input for obstacle avoidance methodologies;
- enhance autonomous deploy/recover procedures, for instance providing feedback for docking;
- create 3D representations for visual inspection, such as the inspection of transition pieces of offshore wind turbines and the scour protection integrity.

As such, by applying the method proposed by Campos et al. [54] to a partial sequence of the ROAM@CRAS it was possible to create a multi-domain map of the harbor. This approach uses the SENSE localization estimation to provide the initial seed of the system state. Then the data acquired through the LiDAR passes through an outlier filter, while the MBES data is georeferenced and concatenated through a predetermined time providing a sliding window that is composed partially by old data, as well as new scans to create an overlap region. The filtered data from both sensors are registered using an ICP-based approach and concatenated to a single representation.

In Figure 24 is depicted the resultant 3D map. From the representation it is possible to observe several moored vessels, as well as the pillars, ramps and walls from the harbor infrastructures. Moreover, the underwater domain map shows the seabed with depths from 1.9-3.0 m, which are in accordance with the official harbor depth rates for the yacht basin.

V. CONCLUSION

This work proposed a modular and multi-domain ASV that provides a research platform for inspection and maintenance tasks capable of acquiring data from both domains, namely surface and underwater. The SENSE is capable of assuming different configurations due to the hardware and software modular design, where changes to the sensor payload, navigation systems, energy availability and localization systems can be made easily. This presents the advantage of providing a testing platform for data acquisition, testing different methodologies and explore new technologies that may emerge throughout time. Moreover, the use of this ASV with multi-domain capabilities will allow to test methods for inspection of the transition pieces, scour protection and

geolocalize submerged structures in projects such as the ATLANTIS.

The use of commercial off-the-shelf materials allows to implement the technology in a cost-effective way, while having a robust mechanical design that can transport an extra payload of 50 kg reaching velocities up to $1.5\,\mathrm{m\,s^{-1}}$. In this paper the hardware and software architectures are introduced, describing each module as well as the interconnections between them in terms of power and communication.

Field tests with SENSE validated the operation and data acquisition capabilities for the surface and underwater domains, as well as the navigation sensors while using the full configuration of the vehicle. This resulted in the creation of the first multi-domain public dataset acquired at biggest port for yachting on the north of Portugal, the *Marina de Leça* harbor. This ROS-compliant dataset provides one complete mission in a fully functional harbor demonstrating several challenges for sensor fusion, tracking, mapping and obstacle detection.

Therefore, this work describes the build composition for each module of the SENSE and makes available a repository with a functional example of the software architecture. Thus, an open-source vehicle is provided which can be easily replicated and allows both research institutes and industries recreate a multi-domain data acquisition platform. Additionally, the public disclosure of the multi-domain dataset offers a powerful tool to develop, validate and test multiple algorithms using real data gathered from a fully functional harbor without the need for the transportation logistics required for a field test.

In the future, the use of new sensors, such as RADAR, the use of different hull types, and the addition of manipulation tecnhologies will allow for even a better situational awareness, a more robust navigation for multiple sea states, and include maintenance capabilities for the transition pieces. Moreover, the navigation control can be improved with the modelation of the external forces applied to the ASV.

REFERENCES

[1] H. Mousazadeh, J. Hamid, O. Elham, M. Farshid, K. Ali, S.-Z. Yousef, and M. Ashkan, "Experimental evaluation of a hydrography surface vehicle in four navigation modes," *J. Ocean Eng. Sci.*, vol. 2, no. 2, pp. 127–136, 2017. [Online]. Available: http://www.sciencedirect.com/science/article/pii/S246801331730027X

[2] D. F. Campos, M. Pereira, A. Matos, and A. M. Pinto, "DIIUS–Distributed perception for inspection of aquatic structures," in *Proc. OCEANS, San Diego–Porto*, Sep. 2021, pp. 1–5. [Online]. Available: https://ieeexplore.ieee.org/document/9705939

[3] P. Leite, R. Silva, A. Matos, and A. M. Pinto, "An hierarchical architecture for docking autonomous surface vehicles," in *Proc. IEEE Int. Conf. Auto. Robot Syst. Competitions (ICARSC)*, Apr. 2019, pp. 1–6. [Online]. Available: https://ieeexplore.ieee.org/document/8733620

[4] R. Silva, P. Leite, D. Campos, and A. M. Pinto, "Hybrid approach to estimate a collision-free velocity for autonomous surface vehicles," in *Proc. IEEE Int. Conf. Auto. Robot Syst. Competitions (ICARSC)*, Apr. 2019, pp. 1–6. [Online]. Available: https://ieeexplore.ieee.org/document/8733643

[5] R. Claro, R. Silva, and A. Pinto, "Detection and mapping of monopiles in offshore wind farms using autonomous surface vehicles," in *Proc. Global Oceans, Singap.–U.S. Gulf Coast*, Oct. 2020, pp. 1–4. [Online]. Available: https://ieeexplore.ieee.org/document/9389348

[6] R. J. Silva, P. Nuno Leite, and A. M. Pinto, "Multi-agent optimization for offshore wind farm inspection using an improved population-based metaheuristic," in *Proc. IEEE Int. Conf. Auto. Robot Syst. Competitions (ICARSC)*, May 2020, pp. 53–60. [Online]. Available: https://ieeexplore.ieee.org/document/9096107

[7] D. F. Campos, A. Matos, and A. M. Pinto, "An adaptive velocity obstacle avoidance algorithm for autonomous surface vehicles," in *Proc. IEEE/RSJ Int. Conf. Intell. Robots Syst. (IROS)*, Nov. 2019, pp. 8089–8096. [Online]. Available: https://ieeexplore.ieee.org/document/8968156

[8] D. F. Campos, A. Matos, and A. M. Pinto, "Multi-domain mapping for offshore asset inspection using an autonomous surface vehicle," in *Proc. IEEE Int. Conf. Auto. Robot Syst. Competitions (ICARSC)*, Apr. 2020, pp. 221–226. [Online]. Available: https://ieeexplore.ieee.org/document/9096097

[9] Z. Liu, Y. Zhang, X. Yu, and C. Yuan, "Unmanned surface vehicles: An overview of developments and challenges," *Annu. Rev. Control*, vol. 41, pp. 71–93, Jan. 2016. [Online]. Available: http://www.sciencedirect.com/science/article/pii/S1367578816300219

[10] M. Breivik, "Topics in guided motion control of marine vehicles," Ph.D. dissertation, NTNU, Trondheim, Norway, 2010. [Online]. Available: https://www.researchgate.net/publication/215523092

[11] R.-J. Yan, S. Pang, H.-B. Sun, and Y.-J. Pang, "Development and missions of unmanned surface vehicle," *J. Mar. Sci. Appl.*, vol. 9, no. 4, pp. 451–457, Dec. 2010, doi: 10.1007/s11804-010-1033-2.

[12] G. N. Roberts and R. Sutton, *Advances in Unmanned Marine Vehicles*. Stevenage, U.K.: IET, Jan. 2006. [Online]. Available: https://digital-library.theiet.org/content/books/ce/pbce069e

[13] G. Eudeline, "Drix USV–improving safety and margins through efficient data acquisition," in *Proc. Abu Dhabi Int. Petroleum Exhib. Conf.*, Nov. 2019, pp. 1–8. [Online]. Available: http://www.onepetro.org/doi/10.2118/197973-MS

[14] B. Bingham, B. Howe, N. Kraus, L. E. Freitag, K. Ball, P. Koski, and E. Gallimore, "Passive and active acoustics using an autonomous wave glider," *J. Field Robot.*, vol. 29, no. 6, pp. 911–923, Nov. 2012, doi: 10.1002/rob.21424.

[15] E. Beck, W. Kirkwood, D. Caress, T. Berk, P. Mahacek, K. Brashem, J. Acain, V. Reddy, C. Kitts, J. Skutnik, and G. Wheat, "SeaWASP: A small waterplane area twin hull autonomous platform for shallow water mapping," *IEEE/OES Auto. Underwater Vehicles*, vol. 43, no. 1, pp. 1–7, Apr. 2008. [Online]. Available: https://ieeexplore.ieee.org/document/5347598

[16] H. Ferreira, C. Almeida, A. Martins, J. Almeida, N. Dias, A. Dias, and E. Silva, "Autonomous bathymetry for risk assessment with ROAZ robotic surface vehicle," in *Proc. Oceans Eur.*, May 2009, pp. 1–6. [Online]. Available: http://ieeexplore.ieee.org/document/5278235/

[17] W.-R. Yang, C.-Y. Chen, C.-M. Hsu, C.-J. Tseng, and W.-C. Yang, "Multifunctional inshore survey platform with unmanned surface vehicles," *Int. J. Autom. Smart Technol.*, vol. 1, no. 2, pp. 19–25, Dec. 2011. [Online]. Available: https://www.ausmt.org/index.php/AUSMT/article/view/122

[18] K. Groves, A. West, K. Gornicki, S. Watson, J. Carrasco, and B. Lennox, "MallARD: An autonomous aquatic surface vehicle for inspection and monitoring of wet nuclear storage facilities," *Robotics*, vol. 8, no. 2, pp. 1–17, Jun. 2019. [Online]. Available: https://www.mdpi.com/2218-6581/8/2/47

[19] J. C. Leedekerken, M. F. Fallon, and J. J. Leonard, "Mapping complex marine environments with autonomous surface craft," in *Experimental Robotics*, 79th ed. Cham, Switzerland: Springer, 2014, pp. 525–539, doi: 10.1007/978-3-642-28572-1_36.

[20] G. Papadopoulos, H. Kurniawati, A. S. B. M. Shariff, L. J. Wong, and N. M. Patrikalakis, "Experiments on surface reconstruction for partially submerged marine structures," *J. Field Robot.*, vol. 31, no. 2, pp. 225–244, Mar. 2014. [Online]. Available: https://onlinelibrary.wiley.com/doi/10.1002/rob.21478

[21] C.-É. N. L. Laflamme, F. Pomerleau, and P. Giguère, "Driving datasets literature review," 2019, *arXiv:1910.11968*.

[22] P. N. Leite, R. J. Silva, D. F. Campos, and A. M. Pinto, "Dense disparity maps from RGB and sparse depth information using deep regression models," in *Lecture Notes in Computer Science (Including Subseries Lecture Notes in Artificial Intelligence and Lecture Notes in Bioinformatics)*, vol. 12131. Cham, Switzerland: Springer, 2021, pp. 379–392, doi: 10.1007/978-3-030-50347-5_33.

[23] P. N. Leite and A. M. Pinto, "Exploiting motion perception in depth estimation through a lightweight convolutional neural network," *IEEE Access*, vol. 9, pp. 76056–76068, 2021. [Online]. Available: https://ieeexplore.ieee.org/document/9438671

[24] A. P. O. Afonso and A. M. Pinto, "Underwater object recognition: A domain-adaption methodology of machine learning classifiers," in *Proc. OCEANS MTS/IEEE Seattle*, Oct. 2019, pp. 1–6. [Online]. Available: https://ieeexplore.ieee.org/document/8962693

[25] M. I. Pereira, "A machine learning approach for predicting docking-based structures," M.S. thesis, Dept. Elect. Comput. Eng., FEUP, Porto, Portugal, 2020. [Online]. Available: https://hdl.handle.net/10216/132609

[26] B. Bovcon, R. Mandeljc, J. Perš, and M. Kristan, "Stereo obstacle detection for unmanned surface vehicles by IMU-assisted semantic segmentation," *Robot. Auton. Syst.*, vol. 104, pp. 1–13, Jun. 2018. [Online]. Available: https://linkinghub.elsevier.com/retrieve/pii/S0921889017305808

[27] A. Pinto and A. C. Matos, "MARESye: A hybrid imaging system for underwater robotic applications," *Inf. Fusion*, vol. 55, pp. 16–29, Mar. 2020. [Online]. Available: https://linkinghub.elsevier.com/retrieve/pii/S156625351830366X

[28] A. M. Pinto, "Atlantis—The Atlantic testing platform for maritime robotics," in *Proc. OCEANS, San Diego–Porto*, 2021, pp. 1–5. [Online]. Available: https://ieeexplore.ieee.org/document/9706059

[29] A. Geiger, P. Lenz, C. Stiller, and R. Urtasun, "Vision meets robotics: The KITTI dataset," *Int. J. Robot. Res.*, vol. 32, no. 11, pp. 1231–1237, 2013. Sep. 2013. [Online]. Available: http://journals.sagepub.com/doi/10.1177/0278364913491297

[30] A. R. Gaspar, A. Nunes, A. M. Pinto, and A. Matos, "Urban@CRAS dataset: Benchmarking of visual odometry and SLAM techniques," *Robot. Auto. Syst.*, vol. 109, pp. 59–67, Nov. 2018. [Online]. Available: https://www.sciencedirect.com/science/article/pii/S0921889018301386

[31] H. Caesar, V. Bankiti, A. H. Lang, S. Vora, V. Erin Liong, Q. Xu, A. Krishnan, Y. Pan, G. Baldan, and O. Beijbom, "NuScenes: A multimodal dataset for autonomous driving," 2019, *arXiv:1903.11027*.

[32] M. Kristan, V. S. Kenk, S. Kovačič, and J. Perš, "Fast image-based obstacle detection from unmanned surface vehicles," *IEEE Trans. Cybern.*, vol. 46, no. 3, pp. 641–654, Mar. 2016. [Online]. Available: https://ieeexplore.ieee.org/document/7073635

[33] C. Li, C. Guo, W. Ren, R. Cong, J. Hou, S. Kwong, and D. Tao, "An underwater image enhancement benchmark dataset and beyond," *IEEE Trans. Image Process.*, vol. 29, pp. 4376–4389, 2020.

[34] K. A. Perrine, K. F. Nieman, T. L. Henderson, K. H. Lent, and T. J. Brudner. (2010). *Five–Element Acoustic Underwater Dataset*. [Online]. Available: http://users.ece.utexas.edu/~bevans/projects/underwater/datasets/ARLUT_01_doc_01.pdf

[35] A. C. Duarte, G. B. Zaffari, R. T. S. da Rosa, L. M. Longaray, P. Drews, and S. S. C. Botelho, "Towards comparison of underwater SLAM methods: An open dataset collection," in *Proc. OCEANS MTS/IEEE Monterey*, Sep. 2016, pp. 1–5. [Online]. Available: https://ieeexplore.ieee.org/document/7761315/

[36] A. Mallios, E. Vidal, R. Campos, and M. Carreras, "Underwater caves sonar data set," *Int. J. Robot. Res.*, vol. 36, no. 12, pp. 1247–1251, Oct. 2017, doi: 10.1177/0278364917732838.

[37] D. F. Duarte, M. I. Pereira, and A. M. Pinto, "Multiple vessel detection and tracking in harsh maritime environments," in *Proc. OCEANS, San Diego–Porto*, Sep. 2021, pp. 1–5. [Online]. Available: https://ieeexplore.ieee.org/document/9705954

[38] B. Bovcon, J. Muhovic, J. Pers, and M. Kristan, "The MaSTr1325 dataset for training deep USV obstacle detection models," in *Proc. IEEE/RSJ Int. Conf. Intell. Robots Syst. (IROS)*, Nov. 2019, pp. 3431–3438. [Online]. Available: https://ieeexplore.ieee.org/document/8967909

[39] M. I. Pereira, A. M. Pinto, and P. N. Leite. (2020). *DORA@CRAS—Docking-Based Structures Dataset*. [Online]. Available: https://rdm.inesctec.pt/dataset/nis-2020-001

[40] M. I. Pereira, R. M. Claro, P. N. Leite, and A. M. Pinto, "Advancing autonomous surface vehicles: A 3D perception system for the recognition and assessment of docking-based structures," *IEEE Access*, vol. 9, pp. 53030–53045, 2021. [Online]. Available: https://ieeexplore.ieee.org/document/9393874

[41] A. Duarte, F. Codevilla, J. D. O. Gaya, and S. S. C. Botelho, "A dataset to evaluate underwater image restoration methods," in *Proc. OCEANS-Shanghai*, Apr. 2016, pp. 1–6. [Online]. Available: http://ieeexplore.ieee.org/document/7485524/

[42] C. Fabbri, M. J. Islam, and J. Sattar, "Enhancing underwater imagery using generative adversarial networks," in *Proc. IEEE Int. Conf. Robot. Autom.*, May 2018, pp. 7159–7165. [Online]. Available: https://ieeexplore.ieee.org/document/8460552/

[43] I. Alonso, M. Yuval, G. Eyal, T. Treibitz, and A. C. Murillo, "CoralSeg: Learning coral segmentation from sparse annotations," *J. Field Robot.*, vol. 36, no. 8, pp. 1456–1477, Dec. 2019. [Online]. Available: https://onlinelibrary.wiley.com/doi/abs/10.1002/rob.21915

[44] E. Gundogdu, B. Solmaz, V. Yücesoy, and A. Koç, "MARVEL: A large-scale image dataset for maritime vessels," in *Lecture Notes in Computer Science (Including Subseries Lecture Notes in Artificial Intelligence and Lecture Notes in Bioinformatics)*, vol. 10115. Cham, Switzerland: Springer, 2016, pp. 165–180. [Online]. Available: http://link.springer.com/10.1007/978-3-319-54193-8_11

[45] N. Cruz, A. Matos, S. Cunha, and S. R. Silva, "Zarco—An autonomous craft for underwater surveys," in *Proc. 7th Geomatic Week*, 2007, pp. 1–8. [Online]. Available: https://hdl.handle.net/10216/69981

[46] T. Moore and D. Stouch, "A generalized extended Kalman filter implementation for the robot operating system," in *Intelligent Autonomous Systems*, vol. 13, E. Menegatti, N. Michael, K. Berns, and H. Yamaguchi, Eds. Cham, Switzerland: Springer, 2016, pp. 335–348, doi: 10.1007/978-3-319-08338-4_25.

[47] J. P. Snyder, "Map projections used by the U.S. Geological survey," U.S. Government Printing Office, Washington, DC, USA, Tech. Rep. 1532, 1982. [Online]. Available: https://pubs.er.usgs.gov/publication/b1532

[48] M. I. Pereira, P. N. Leite, and A. M. Pinto, "Detecting docking-based structures for persistent ASVs using a volumetric neural network," in *Proc. Global Oceans, Singap.–U.S. Gulf Coast*, 2020, pp. 1–6. [Online]. Available: https://ieeexplore.ieee.org/document/9389349

[49] N. Wawrzyniak, T. Hyla, and A. Popik, "Vessel detection and tracking method based on video surveillance," *Sensors*, vol. 19, no. 23, p. 5230, Nov. 2019. [Online]. Available: https://www.mdpi.com/1424-8220/19/23/5230

[50] L. Steccanella, D. D. Bloisi, A. Castellini, and A. Farinelli, "Waterline and obstacle detection in images from low-cost autonomous boats for environmental monitoring," *Robot. Auto. Syst.*, vol. 124, Feb. 2020, Art. no. 103346. [Online]. Available: https://linkinghub.elsevier.com/retrieve/pii/S0921889019302775

[51] D. F. Campos, P. N. Leite, S. Renato, M. I. Pereira, R. Claro, and A. M. Pinto, "ROAM@CRAS—A harbor multidomain mapping dataset," INESC TEC Res. Data Repository, Sep. 2020. [Online]. Available: https://rdm.inesctec.pt/dataset/nis-2020-002

[52] Y. M. Wang, Y. Li, and J. B. Zheng, "A camera calibration technique based on OpenCV," in *Proc. 3rd Int. Conf. Inf. Sci. Interact. Sci.*, Jun. 2010, pp. 403–406. [Online]. Available: http://ieeexplore.ieee.org/document/5534797

[53] A. Dhall, K. Chelani, V. Radhakrishnan, and K. M. Krishna, "LiDAR-camera calibration using 3D-3D point correspondences," 2017, *arXiv:1705.09785*.

[54] D. F. Campos, A. Matos, and A. M. Pinto, "Multi-domain inspection of offshore wind farms using an autonomous surface vehicle," *Social Netw. Appl. Sci.*, vol. 3, no. 4, p. 455, Apr. 2021. [Online]. Available: http://link.springer.com/10.1007/s42452-021-04451-5

[55] C. Forster, M. Pizzoli, and D. Scaramuzza, "Svo: Fast semi-direct monocular visual odometry," in *Proc. IEEE Int. Conf. Robot. Autom.*, Apr. 2014, pp. 15–22. [Online]. Available: http://ieeexplore.ieee.org/document/6906584/

[56] B. Teixeira, H. Silva, A. Matos, and E. Silva, "Deep learning for underwater visual odometry estimation," *IEEE Access*, vol. 8, pp. 44687–44701, 2020. [Online]. Available: https://ieeexplore.ieee.org/document/9024043/

[57] E. Skjellaug, E. F. Brekke, and A. Stahl, "Feature-based laser odometry for autonomous surface vehicles utilizing the point cloud library," in *Proc. IEEE 23rd Int. Conf. Inf. Fusion (FUSION)*, Jul. 2020, pp. 1–8. [Online]. Available: https://ieeexplore.ieee.org/document/9190370/

[58] Z. Zhang and D. Scaramuzza, "A tutorial on quantitative trajectory evaluation for visual(-inertial) odometry," in *Proc. IEEE/RSJ Int. Conf. Intell. Robots Syst. (IROS)*, Madrid, Spain, Oct. 2018, pp. 7244–7251. [Online]. Available: https://ieeexplore.ieee.org/document/8593941

DANIEL FILIPE CAMPOS received the M.Sc. degree in electrical and computer engineering from the Faculty of Engineering of the University of Porto (FEUP), Portugal, in 2014, where he is currently pursuing the Ph.D. degree with the Department of Electrical and Computer Engineering. He did his Ph.D. degree with the Ph.D. Research Studentships from FCT. He is currently a Researcher at the Centre for Robotics and Autonomous Systems (CRAS), INESC TEC. His current research interests include robotics, multi-domain mapping, distributed perception, and collision avoidance techniques, mainly focused on maritime scenarios.

ANÍBAL MATOS (Member, IEEE) received the Ph.D. degree in electrical and computer engineering from Porto University, in 2001. He is currently an Associate Professor at the Faculty of Engineering of Porto University and a member of the Board of Director at the INESC TEC. His research interests include perception, sensing, navigation, and control of autonomous marine robots, being the author or coauthor of more than 80 publications in international journals and conferences. He has participated and lead several research projects on marine robotics and its application to monitoring, inspection, search and rescue, and defense.

ANDRY MAYKOL PINTO received the Ph.D. degree in electrical and computer engineering from the Faculty of Engineering of University of Porto, Portugal, in 2014. He is currently an Assistant Professor at the Faculty of Engineering of University of Porto and a Senior Researcher at the Centre for Robotics and Autonomous Systems, INESC TEC. He is the Principal Investigator of national and international research and development projects related to robotic-based operation and maintenance (O&M) activities for offshore infrastructures. His research interests include multi-domain perception, underwater imaging, artificial intelligence, and mobile robotics.